J. Fluid Mech. (1999), *vol.* 387, *pp.* 97–127. Printed in the United Kingdom

© 1999 Cambridge University Press

Shear instability in shallow water

By N. J. BALMFORTH

Scripps Institution of Oceanography, University of California, La Jolla, CA 92093-0230, USA

(Received 11 February 1998 and in revised form 17 November 1998)

This study considers the linear stability of shear flows in shallow water. It explores instabilities related to the classical incompressible (Rayleigh) instability, and those caused by the over-reflection of surface gravity waves. Numerical solutions of the linear stability problem are presented, together with analytical arguments elucidating the role of finite potential vorticity gradients. The slow development of marginally unstable modes is considered for almost inviscid flows. This is described by an evolution equation for the amplitude of the unstable mode, coupled to a critical-layer potential vorticity equation. This reduced system presents a compact description of the linear stability problem and allows exploration of viscous effects.

1. Introduction

Shear instability plays a fundamental role in a variety of fluid mechanical phenomena in the astro- and geosciences. The particular problem under discussion here is shear instability in a shallow fluid layer at high Reynolds number. This problem has applications to a variety of flows in geophysics (Satomura 1981; Griffiths, Killworth & Stern 1982; Kubokawa 1985; Hayashi & Young 1987), and accretion and pattern forming processes in astrophysical disks (Drury 1985; Glatzel 1985; Narayan, Goldreich & Goodman 1987; Papaloizou & Pringle 1987). The shallow water system is analogous to a two-dimensional compressible flow, and so the problem also has a slightly different interpretation.

It is known that inviscid shear flows in shallow water (or two-dimensional compressible fluid) may suffer two types of instability (Blumen, Drazin & Billings 1975). The first is closely related to the classical Rayleigh instability of incompressible flows (Rayleigh 1880). When the fluid is effectively incompressible (of small Froude number) and of constant mean depth (density), one expects this classical form of instability to remain relatively unmodified. That is, under the usual conditions of the Rayleigh–Fjortoft theorem (Rayleigh 1880; Fjørtoft 1950), to exist when there are inflection points in the flow 'profile' $U(y)$, where y is the cross-stream coordinate. In this paper, this first kind of instability will be refered to as 'inflectional instability'.

Shallow water shear flows can also be unstable to a second type of instability related to surface gravity waves (Satomura 1981; for compressible flows the instability is connected to acoustic waves – Broadbent & Moore 1979; Blumen *et al.* 1975). The underlying physical mechanism has been interpreted as an over-reflection process, or as the coupling of positive and negative energy modes (Takehiro & Hayashi 1992). Here, this second form of instability will be referred to as 'supersonic', since in order to exist the wave speed must match the mean fluid velocity somewhere in the flow.

The aim of the current work is two-fold. First, a complete description of linear

https://doi.org/10.1017/S0022112099004279 Published online by Cambridge University Press

stability is presented. This includes an analysis of the effects of gradients in the background potential vorticity (which are often neglected in this context; but see Drury 1985; Kubokawa 1985; Papaloizou & Pringle 1987; Perkins & Renardy 1997) and weak viscosity. The second aim is to construct a perturbation theory for marginally unstable, almost inviscid flows. This extends previous work on shallow water and compressible flows by advancing into the viscous and nonlinear regimes, and provides the compressible version of theories of marginally stable, incompressible, inviscid shears (Stewartson 1981; Balmforth & Young 1997). Previously, Shukhman (1991) and Williams (1992) have given weakly nonlinear theories of acoustic instabilities of vortices. These studies are related to the current one, but Shukhman derives an amplitude equation containing an infinite sum, and Williams particularizes to flows with constant potential vorticity and ignores critical-layer effects.

2. Formulation of the problem

Consider a channel containing a shallow fluid layer with equilibrium velocity profile, $U(y)$, and depth, $H(y)$. Here, $U(y)$ and $H(y)$ are arbitrary functions, but in this study, $U(y)$ will be assumed to be a monotonic function. Disturbances to this state are governed by the dimensionless equations,

$$(\partial_t + U\partial_x)u + U'v + uu_x + vu_y = -\frac{1}{F^2}h_x + \frac{\epsilon^3\nu}{(H+h)}\{\partial_x[(H+h)u_x] + \partial_y[(H+h)u_y]\}, \quad (2.1)$$

$$(\partial_t + U\partial_x)v + uv_x + vv_y = -\frac{1}{F^2}h_y + \frac{\epsilon^3\nu}{(H+h)}\{\partial_x[(H+h)v_x] + \partial_y[(H+h)v_y]\} \quad (2.2)$$

and

$$(\partial_t + U\partial_x)h + \partial_x[(H+h)u] + \partial_y[(H+h)v] = 0, \quad (2.3)$$

solved on the domain, $-\infty < x < \infty$ and $-1 < y < 1$. In (2.1)–(2.3) the nondimensionalization leaves the Froude number, F, a parameter equivalent to a characteristic Mach number, but based on the surface gravity wave speed rather than sound speed. In addition, the velocity profile and height field have characteristic values of unity: $U(\pm 1) = \pm 1$ and $H(0) = 1$. The equations also include viscous terms with dimensionless coefficient, $\epsilon^3\nu$; the factor ϵ is a small parameter that will be exploited later (the scaling of ϵ^3 is a distinguished one and ensures the flow is nearly inviscid). In the circumstance that $\nu = 0$, any $U(y)$ is an equilibrium; when $\nu \neq 0$, the arbitrary velocity profile $U(y)$ must be maintained by a suitable body force.†

Equations (2.1)–(2.3) are solved subject to boundary conditions of no flow at the walls, $v(x, \pm 1, t) = 0$. In addition, when $\epsilon^3\nu \neq 0$, no slip should also be imposed on the velocity field. However, in the problem at hand, the viscous terms will only become important inside the interior in special slender regions (the critical layers) and in wall boundary layers; the effect of viscosity decays exponentially quickly outside these layers and the viscous boundary condition decouples from the interior problem. Hence, explicit consideration of the no-slip condition is not necessary.

† Note that the viscous terms are energetically consistent, but may not be the proper dissipative terms for a shallow water theory. However, viscosity will only be considered as a perturbation of the inviscid problem, and in the asymptotic expansion only simplified forms of the dissipative terms appear; the precise, original form is unimportant.

https://doi.org/10.1017/S0022112099004279 Published online by Cambridge University Press

3. Inviscid linear theory

Before constructing any weakly nonlinear theory, it is first necessary to provide a complete discussion of linear stability. In the current context, previous work has covered a substantial amount of the linear stability theory. However, most of this work has concentrated upon flows with constant potential (specific) vorticity (Satomura 1981; Hayashi & Young 1987; Narayan *et al.* 1987; Takehiro & Hayashi 1992). This leads to a crucial simplification in the normal mode problem. Here, this restriction will be relaxed.

The equations for normal modes with dependence $\exp \mathrm{i}k(x-ct)$ take the form

$$\mathrm{i}k(U-c)u + U'v = -\frac{\mathrm{i}k}{F^2}h, \tag{3.1}$$

$$\mathrm{i}k(U-c)v = -\frac{1}{F^2}h_y \tag{3.2}$$

and

$$\mathrm{i}k(U-c)h + \mathrm{i}kHu + (Hv)_y = 0. \tag{3.3}$$

The elimination of u and h leads to the second-order equation

$$\partial_y\left[\frac{1}{HK^2}\partial_y(Hv)\right] - v + \frac{k^2F^2U'}{K^4}\left[2Q + \frac{H'}{H^2}(U-c)\right]v + \frac{HQ'v}{K^2(U-c)} = 0, \tag{3.4}$$

where

$$K^2 = k^2\left[1 - \frac{F^2}{H}(U-c)^2\right] \tag{3.5}$$

and $Q = -U'/H$ is the background potential vorticity.

The normal-mode equation (3.4) has two kinds of singular points. The first arises where $K^2 = 0$, or, equivalently, when $y = y_t$ with

$$U(y_t) = c \pm H^{1/2}/F. \tag{3.6}$$

These points may be identified as the turning points of short-wavelength waves, and are removable (this is seen on writing the system as two first-order equations for u and v; then there are no singular coefficients at $y = y_t$). The second singular point occurs where $y = y_c$ with $U(y_c) = c$. For monotonic velocity profiles (which will be considered), there is only one such singular point. This is the so-called *critical level* of a wave-like disturbance with (real) wave speed c. Unless $Q' = 0$ everywhere, the critical-level singularity cannot be removed (hence to avoid the attendant complications, $Q' = 0$ was often assumed in previous discussions).

Here, the equations will be solved specifically for various model flow profiles with $H = 1$. One particular family is given by

$$U(y) = \frac{\tanh \alpha y}{\tanh \alpha}. \tag{3.7}$$

The numerical scheme used is based on a Newton–Raphson–Kantorovitch algorithm (Cash & Singhal 1982). This algorithm is not specially designed for problems with potentially singular points, and spurious neutral eigenvalues occasionally arise in using it. To improve the detection of these fake eigenvalues, additional grid points were placed at and around the critical level.

https://doi.org/10.1017/S0022112099004279 Published online by Cambridge University Press

3.1. *Conservation laws*

Three important relations for the inviscid system are the following; these are quoted specifically for the case $H = 1$.

First, the inviscid potential vorticity equation is

$$(\partial_t + U\partial_x)q + uq_x + vq_y + Q'v = 0, \tag{3.8}$$

where

$$Q + q = -\frac{U' + u_y - v_x}{1 + h}. \tag{3.9}$$

In linear theory, this equation becomes

$$\mathrm{i}k(U - c)q + Q'v = 0, \tag{3.10}$$

where

$$q = -(u_y - v_x + Qh). \tag{3.11}$$

Second, the energy equation of inviscid linear theory takes the form

$$\frac{\mathrm{d}E}{\mathrm{d}t} = \frac{1}{2}\int_{-1}^{1} U(v^*q + vq^*)\mathrm{d}y, \tag{3.12}$$

where

$$E = \frac{1}{2}\int_{-1}^{1} [|u|^2 + |v|^2 + F^{-2}|h|^2 + U(u^*h + h^*u)]\mathrm{d}y. \tag{3.13}$$

Third, the total streamwise momentum balance is

$$\frac{\mathrm{d}M}{\mathrm{d}t} = -\frac{1}{2}\int_{-1}^{1} (v^*q + vq^*)\mathrm{d}y, \tag{3.14}$$

with

$$M = \frac{1}{2}\int_{-1}^{1} (u^*h + h^*u)\mathrm{d}y. \tag{3.15}$$

4. Numerical calculations

4.1. *Inflectional instability*

When $F = 0$, the surface gravity wave speed becomes infinite and these waves are filtered from the problem. The normal-mode equation in that circumstance reduces to

$$\partial_y\left[\frac{1}{H}\partial_y(Hv)\right] - k^2v + \frac{HQ'v}{U - c} = 0, \tag{4.1}$$

which may be described as an 'anelastic' version of Rayleigh's equation. Importantly, an analogue of the Rayleigh–Fjortoft Theorem follows for this system: instability can only exist if Q possesses a local minimum somewhere within the flow (assuming $U' > 0$).

Another important feature of equation (4.1) is that it admits neutral solutions only if either $v(y_c) = 0$, or if $Q'(y_c) = 0$, where y_c is the critical level of the neutral mode. But one can show that solutions for which $v(y_c) = 0$ do not satisfy the boundary conditions (this does not remain the case for the general normal-mode equation; some solutions with $v(y_c) = 0$ are displayed in the next subsection). Hence, neutral modes can only exist if their critical level aligns with an inflection point.

https://doi.org/10.1017/S0022112099004279 Published online by Cambridge University Press

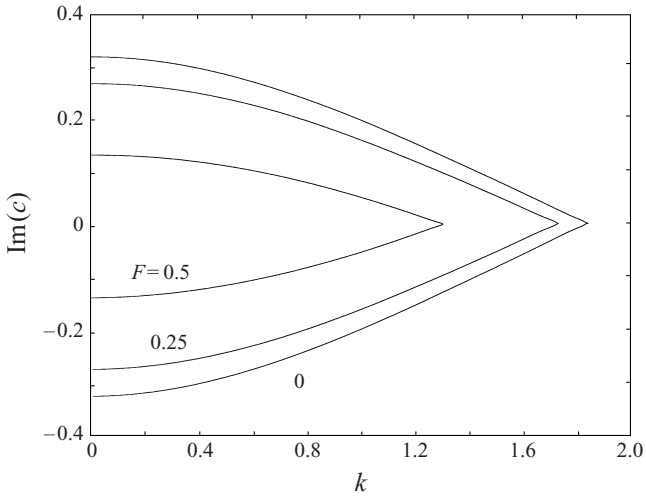


FIGURE 1. Inflectional instability for three values of F (0, 0.25 and 0.5; see labels) and $\alpha = 2$. Shown is c_i against k.

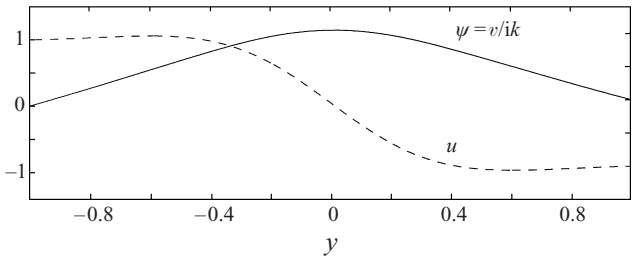


FIGURE 2. Eigenfunctions of the neutral mode at the edge of the unstable band of wavenumbers; $k = k_m \approx 1.303$, $F = 0.5$ and $\alpha = 2$.

For the model flow (3.7), the criterion for instability is satisfied and so the shear is potentially unstable. This is verified by numerical computations, which are shown in figure 1. This figure displays growth and decay rates for the anelastic case, $F = 0$, and for two finite values of F.

Complex eigenmodes appear as conjugate pairs, corresponding to growing and decaying modes, and the unstable band of wavenumbers occupies the range $0 < k < k_c$. At $k = k_c$, there is a neutral mode whose critical level lines up with the inflection point ($y = 0$); the eigenfunction is illustrated in figure 2 for $F = 0.5$ and $\alpha = 2$. Evidently, compressibility (the divergence of the velocity field) exerts a stabilizing role, as found previously by Blumen (1970) and Blumen *et al.* (1975).

Another remarkable feature of the inflectional instability is that for $k > k_c$ there are no discrete eigenmodes connected to the unstable modes. This reflects the fact that the modes bifurcate from a continuous spectrum consisting of wave speeds c in the range $[-1, 1]$ (the range of flow speeds, e.g. Case 1960). In a standard Hamiltonian problem there would normally be two neutral modes to the stable side of the point of bifurcation (in k), but here there is only this continuous spectrum.

For $F \neq 0$, there is also an infinite number of surface gravity waves. However, provided that F is small, these waves all have phase speeds that lie outside the range of flow speeds, $[-1, 1]$ (see figure 3). Moreover, they are always stable. When F

https://doi.org/10.1017/S0022112099004279 Published online by Cambridge University Press

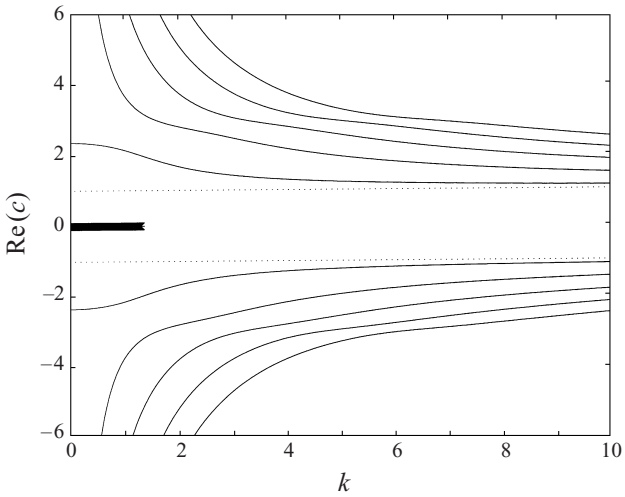


FIGURE 3. Wave speeds of the surface gravity modes for $F = 0.5$ and $\alpha = 2$. The thick line indicates the unstable modes.

becomes sufficiently large, however, these modes can acquire phase speeds that match the flow speed somewhere within the channel. That is, they acquire critical levels. In this circumstance, the modes can become unstable.

4.2. *Supersonic instabilities*

When $\alpha = 0$, the velocity profile becomes linear (Couette flow), there is no background vorticity gradient, and the critical level does not present a singularity in the normal-mode equation. In fact, that equation is written most compactly in terms of u:

$$u_{yy} - k^2[1 - F^2(y - c)^2]u = 0, \tag{4.2}$$

which has parabolic cylinder functions as solutions (Narayan *et al.* 1987). In such a situation, inflectional instability is impossible, and there remains only the surface gravity waves that may be destabilized through over-reflection (Satomura 1981; Takehiro & Hayashi 1992).

In figure 4, the (complex) wave speed is shown for the case $\alpha = 0$ and $F = 2$. The surface gravity waves have phase speeds that enter the range of flow speeds once k becomes sufficiently large. The picture portrayed in figure 4 reproduces the results of Satomura (1981) and Takehiro & Hayashi (1992). Figure 5 shows the eigenfunctions of the neutrally stable modes bounding the instability band with lowest wavenumber. Note how the symmetry changes from one side of the instability band to the other. Also, the mode shown in figure 5(b) is one of a small subset of the modes for which $v(y_c) = 0$.

The pattern of the wave speed shown in figure 4(a) can be roughly understood using short-wavelength arguments. The modal dispersion relation is, in this approximation,

$$\tan\phi_+ \tan\phi_- \sim \tfrac{1}{4}\mathrm{e}^{-\Phi} \tag{4.3}$$

(cf. Knessl & Keller 1992; Ford 1994), where

$$\phi_+ = k\int_{y_+}^{1} [F^2(U-c)^2 - 1]^{1/2}\mathrm{d}y, \quad \phi_- = k\int_{-1}^{y_-} [F^2(c-U)^2 - 1]^{1/2}\mathrm{d}y \tag{4.4}$$

https://doi.org/10.1017/S0022112099004279 Published online by Cambridge University Press

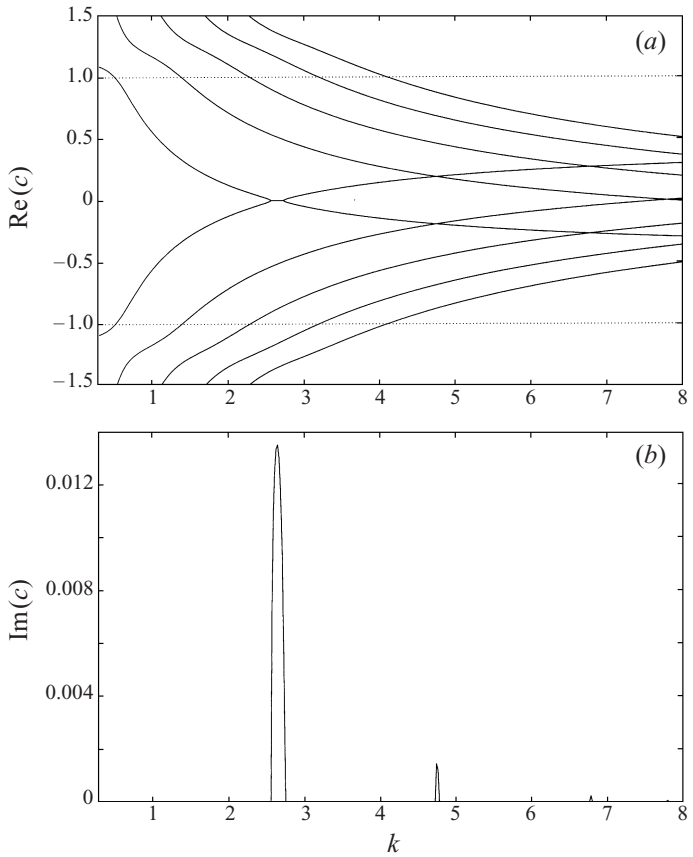


FIGURE 4. Supersonic instability when $\alpha = 0$ and $F = 2$: (*a*) wave speed, c_r, and (*b*) c_i against k for the five lowest-order pairs of surface gravity waves.

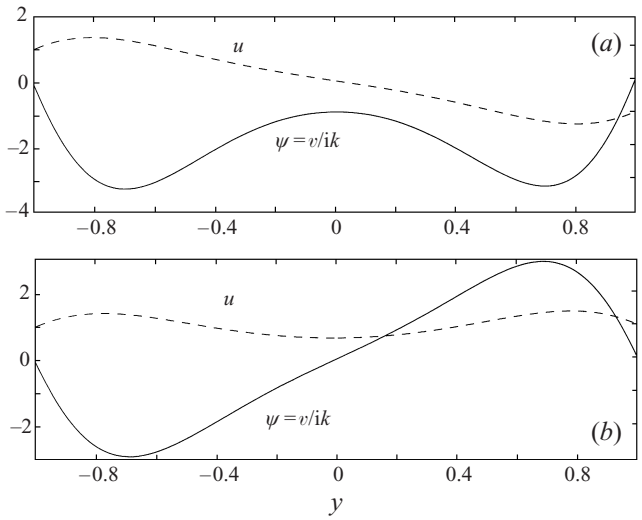


FIGURE 5. Eigenfunctions of the neutral modes at the edges of the lowest-wavenumber instability band; (*a*) $k = k_b \approx 2.73235$ and (*b*) $k = k_a \approx 2.5573$. $F = 2$ and $\alpha = 0$.

https://doi.org/10.1017/S0022112099004279 Published online by Cambridge University Press

and

$$\Phi = k\int_{y_-}^{y_+}[1-F^2(U-c)^2]^{1/2}\mathrm{d}y, \tag{4.5}$$

with $y_\pm$ denoting the two turning points in (3.6), provided these lie inside the channel.

The right-hand side of (4.3) is exponentially small in the short-wavelength limit, and so the dispersion relation simplifies to

$$\phi_+ \sim n\pi \quad \text{or} \quad \phi_- \sim n\pi, \quad \text{with } n = 1, 2, \ldots. \tag{4.6}$$

These two pieces of the dispersion relation reveal the presence of two sets of surface gravity modes, one set concentrated in the region $[y_+, 1]$, the other in $[-1, y_-]$. The corresponding eigenvalues comprise the two sets of interweaving branches of wave speeds in figures 3 and 4. However, though (4.6) describes the pattern of interweaving branches, it does not predict the instability bands that open up when the branches cross. These bands occur when both of (4.6) hold simultaneously. In that circumstance, (4.3) may be expanded in another way:

$$c_i^2 = \frac{1}{4k^4F^4}\mathrm{e}^{-\Phi}\left[\int_{-1}^{y_-}\frac{(c-U)\mathrm{d}y}{[F^2(U-c)^2-1]^{1/2}}\int_{y_+}^{1}\frac{(U-c)\mathrm{d}y}{[F^2(U-c)^2-1]^{1/2}}\right]^{-1}. \tag{4.7}$$

This indicates that the peak in c_i in each instability band is a rapidly decreasing function of k (as in figure 4*b*).

The instability displayed in figure 4 can be rationalized as coupling between waves with different senses of wave action or energy (Hayashi & Young 1987; Takehiro & Hayashi 1992). On substituting the normal-mode form into equation (3.15) and assuming c to be real, it follows that, when $\alpha = 0$,

$$M = -\frac{k^2F^2}{2(k^2+F^2)}\int_{-1}^{1}(U-c)|u|^2\mathrm{d}y. \tag{4.8}$$

For a particular mode, M can be identified as the disturbance momentum and, for $\alpha = 0$, used as an alternative to action (Takehiro & Hayashi 1992). Modes that are concentrated above the critical level have eigenfunctions for which $|u|^2$ is strongly localized to the region $[y_+, 1]$, in which $U > c$. Hence these modes have negative disturbance momentum. The modes concentrated below the critical level have $U < c$ in the regions in which they are localized, and so they have positive disturbance momentum. In other words, the modes that appear at small k with positive phase speed have $M > 0$, and those with negative phase speed have $M < 0$. (Another way of observing these modal properties is through the relation

$$F^2k^3\frac{\partial c}{\partial k}\int_{-1}^{1}(U-c)|u|^2\mathrm{d}y = \int_{-1}^{1}|u_y|^2\mathrm{d}y, \tag{4.9}$$

obtained from (4.2), which indicates that $\partial c/\partial k \propto -M^{-1}$. Hence from figure 4 the sign of M can be read off.) When the phase speeds of the two types of modes cross, there is an interaction in which each of the modes fuels the other to give rise to an exponentially growing disturbance.

An important feature of the dispersion relation (4.6) is that as $k \to \infty$ with n fixed, either $y_+ \to 1$ or $y_- \to -1$ (since $\phi_\pm$ must remain finite). That is, $c \to -1 + F^{-1}$ or $c \to 1 - F^{-1}$ for the 'upper' or 'lower' branches respectively. For $F = \frac{1}{2}$, the branches accumulate to $c = \pm 1$, as in figure 3; for $F = 2$, the accumulation speeds are $\pm\frac{1}{2}$ (figure 4).

https://doi.org/10.1017/S0022112099004279 Published online by Cambridge University Press

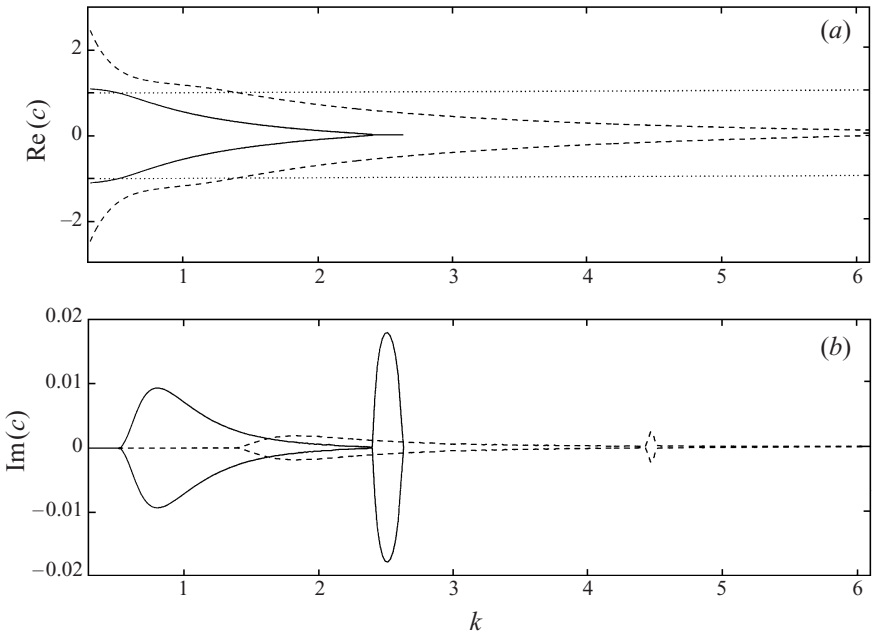


FIGURE 6. Supersonic instability when $\alpha = 0.5$ and $F = 2$. The two lowest-order pairs of surface gravity waves are shown. (*a*) Wave speed, c_r, and (*b*) c_i against k.

The two sets of branches therefore will only cross when $1-F^{-1} > 0$ and $-1+F^{-1} < 0$; equivalently, $F > 1$. Importantly, in this circumstance, all the branches cross, and so there must be an infinite number of instability bands. This is a necessary condition for instability, and is stronger than the requirement that the flow be supersonic (Blumen 1970; Ripa 1983), which is $F > \frac{1}{2}$ (cf. figure 3). The improvement in this condition arises because $F > 1$ recognizes that mode coupling must occur, whereas $F > \frac{1}{2}$ ensures only that there is a critical layer. When the flow has potential vorticity gradients, however, $F > \frac{1}{2}$ is the more appropriate condition because only the existence of a critical layer is needed for instability, as will become clear shortly.

If one concentrates on the crossings at $c = 0$, then (4.6) predicts the resonant wavenumber, $k = k_r$ with

$$k_r \sim n\pi \left[\int_{1/F}^{1} (F^2U^2 - 1)^{1/2} \, \mathrm{d}y \right]^{-1}. \tag{4.10}$$

Thus, the crossings become equally spaced once k is sufficiently large. In other words, when the flow loses stability, there are resonant chains of unstable modes, a feature that is important in any nonlinear theory.

4.3. *The effect of potential vorticity gradients*

When $\alpha \neq 0$, the critical-level singularity fundamentally affects the problem. Again, one can show that modes can only be neutral if $v(y_c) = 0$ or $Q'(y_c) = 0$. This condition places an important constraint on the location of the neutral modes. In particular, as indicated by the numerical results displayed in figures 6–9, it forces most of the neutral modes possessing critical levels to either split into growing/decaying mode pairs or entirely disappear.

In the current problem one can employ the energy and momentum equations (3.12)

https://doi.org/10.1017/S0022112099004279 Published online by Cambridge University Press

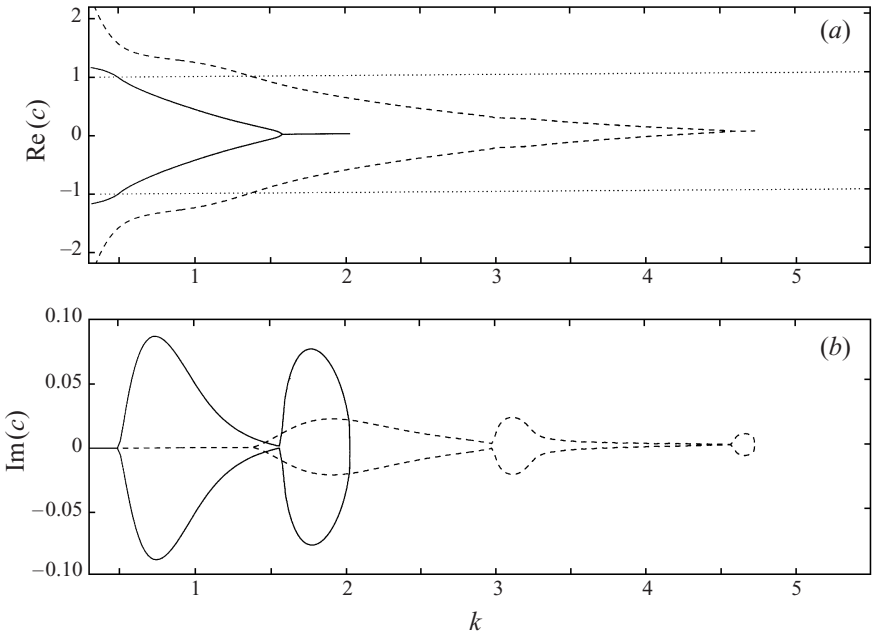


FIGURE 7. As figure 6 but for $\alpha = 2$.

and (3.14) to rationalize this effect of the critical-level singularity. If Q' is everywhere small, then (3.12) and (3.14) can be rewritten in the forms

$$|c_i| = -\frac{\pi c Q_c' |v_c|^2}{2k^2 E |U_c'|} \quad \text{and} \quad |c_i| = \frac{\pi Q_c' |v_c|^2}{2k^2 M |U_c'|} \tag{4.11}$$

(cf. Kubokawa 1985), where the subscript c indicates the value at the critical level. (This relation also implies $E = -cM$.) Thus, provided $-cQ_c'/E$ or Q_c'/M is positive, there is a growing and decaying pair of modes. However, if Q_c'/M is negative, equation (4.11) is inconsistent and there can be no normal modes. The existence of unstable modes therefore hinges on the sign of the combination Q_c'/M. For modes with $M > 0$, instability exists in regions with positive potential vorticity gradient. But there are no modes where that gradient is negative. The opposite is true for modes with $M < 0$.

This explains the instability and disappearance of modes in figures 6 and 7 (cf. Perkins & Renardy 1997). In these pictures, the lowest-order surface gravity modes enter the range of flow speeds and immediately become unstable. This is just a consequence of the fact that $Q' \equiv -U'' < 0$ near $y = -1$ where the modes with $M < 0$ enter the critical-level region, and $Q'(y) > 0$ where the $M > 0$ modes enter the range of flow speed. Subsequently, the modes collide at the inflection point, $y = 0$, and the modal interaction again occurs, generating the 'bubble' in c_i. However, when the interaction ceases at larger k ($k > 2.6$ in figure 6 and $k > 2$ for the lowest order mode in figure 7), both modes disappear because their critical levels enter regions in which $Q_c'/M < 0$.

One physical image of the destabilization by potential vorticity gradients is that when $Q'(y)$ is finite, the critical level emits wave action and drives the modes if $Q'/M > 0$ (Drury 1980). When $Q'/M < 0$, on the other hand, the critical level is 'absorbing'. The physical interpretation is incomplete because, when the critical level

https://doi.org/10.1017/S0022112099004279 Published online by Cambridge University Press

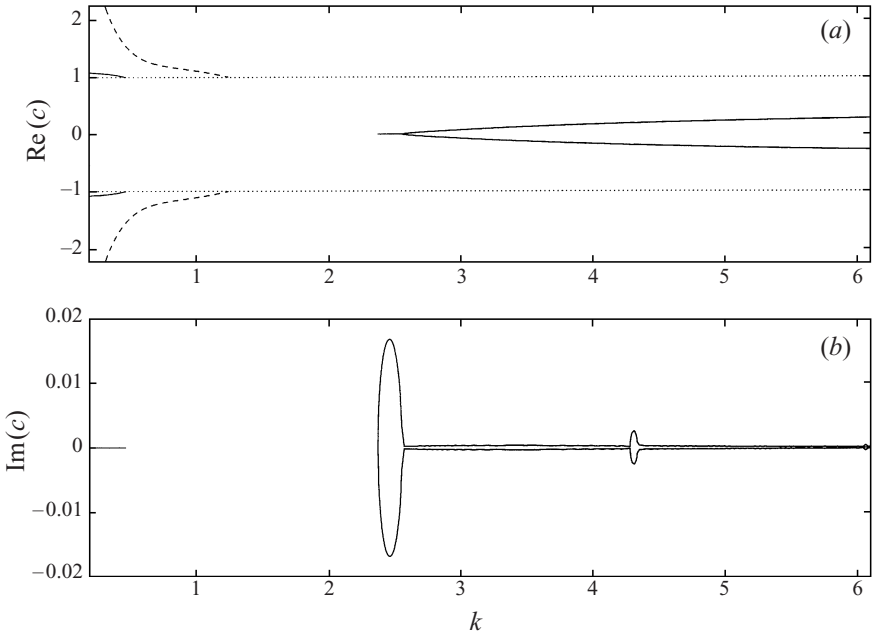


FIGURE 8. Supersonic instability for the model flow, $U(y) = (y + 0.1y^3)/1.1$ and $H(y) = 1$ with $F = 2$. The two lowest-order pairs of surface gravity waves are shown. (*a*) Wave speed, c_r, and (*b*) c_i against k.

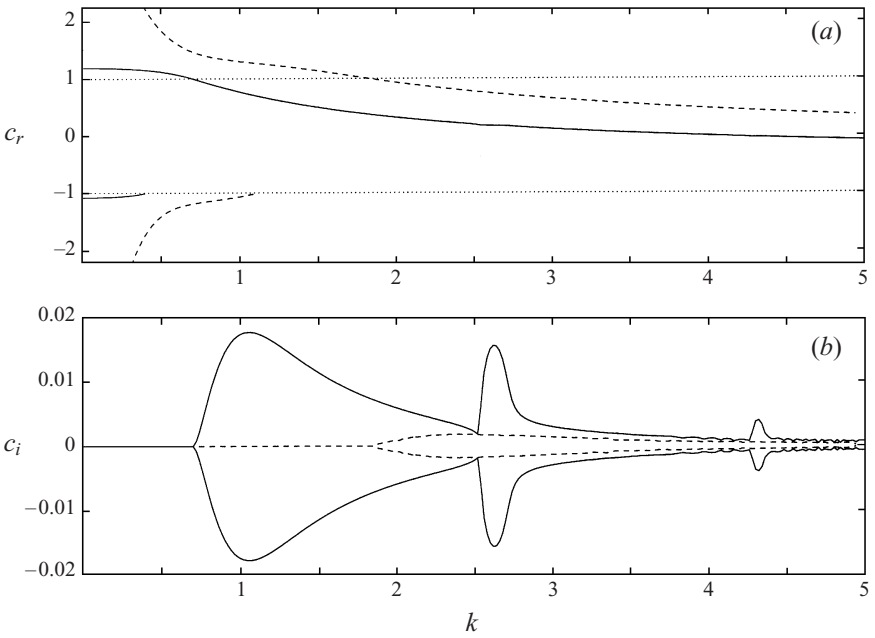


FIGURE 9. Supersonic instability for the model flow, $U(y) = y - 0.3(y^2 - 1)$ and $H(y) = 1$ with $F = 2$. The two lowest-order 'pairs' of surface gravity waves are shown (these are no longer symmetrical under $c_r \to -c_r$ since the profile is no longer symemtrical under $y \to -y$). (*a*) Wave speed, c_r, and (*b*) c_i against k.

https://doi.org/10.1017/S0022112099004279 Published online by Cambridge University Press

'absorbs' wave action, modes disappear rather than become damped, and when it is 'emitting' there is also a decaying mode.

More solutions of the linear stability problem are illustrated in figures 8 and 9, which show the wave speed of the lowest-order surface gravity waves for model flows with $U(y) = (y + 0.1y^3)/1.1$ and $U(y) = y - 0.3(y^2 - 1)$, respectively (and $H = 1$). In the first case, the sense of the potential vorticity gradient is exactly the opposite to that of the tanh profile used for figures 6 and 7. As a result, the modes are destabilized or disappear in precisely the converse fashion to the hyperbolic case: the modes disappear when they first enter the critical level region at small k, then reappear at larger k beyond the first modal interaction. In the second example, Q' is constant and positive. Consequently, the modes entering the range of flow speeds from above continue to exist as conjugate pairs. Those that approach $c = -1$ from below disappear once they acquire critical levels.

The disappearance of the modes also affects the modal resonances away from the inflection point ($y = 0$). Because of critical-level singularity, one of the interacting modes now no longer exists, and so these resonances cannot occur. However, there remains a remnant of the interaction that leads to a sharp peak in the growth rates (e.g. $k = 4.5$ in figure 6, $k = 3.1$ in figure 7 and $k = 4.4$ in figures 8 and 9).

At first sight it seems peculiar that a modal quartet (two pairs of growing/decaying modes) can appear in place of a pair of neutral surface gravity waves as soon as the potential vorticity is non-zero. However, the key point is that the neutral modes are embedded in the continuous spectrum. If the background potential vorticity is uniform, this continuous spectrum is not coupled to the surface gravity waves. But when the potential vorticity gradient is finite, the surface gravity modes couple to the continuum. The extra eigenvalues that appear can be interpreted as arising from the continuous spectrum (they are 'resonance poles' that move off a different Riemann sheet of the dispersion relation and onto the physical spectral plane as the potential vorticity gradient is introduced – see, for example, Crawford & Hislop 1989).

5. Critical-layer expansions: weakly nonlinear, inflectional modes

Next, some analytical developments of the problem are explored that are related to the critical-layer expansions often used for Rossby waves (Stewartson 1978; Warn & Warn 1978) and in spatially developing flows (Goldstein & Leib 1988; Goldstein & Hultgren 1988). The aim is two-fold.

The expansions are part of the weakly nonlinear theory of instabilities in the problem. The calculation can be carried through without difficulty for the inflectional instabilities (this case is dealt with first in this section; see also Appendix A). But there are some difficulties with the theory for supersonic instabilities, as will be described in the next section. The second point of the expansions is that they provide analytical insights into the linear stability problem, which is the main theme of this paper. Notably, this insight extends to the slightly viscous problem, and consequently the rather unusual effects of viscosity on the normal modes can be uncovered.

5.1. *The expansion*

Figure 1 indicates that the band of unstable wavenumbers occupies a range $[0, k_c]$. At this stage it is possible to proceed in one of two ways. If the system is spatially extended, then a weakly nonlinear expansion would be opened once one of the parameters α and F were tuned such that the band shrank to $k = 0$. This situation is similar to that considered by Balmforth & Young (1997). The second route is

https://doi.org/10.1017/S0022112099004279 Published online by Cambridge University Press

to consider purely periodic systems in which there is a minimal wavenumber, k_m. If $k_m = k_c$, the periodic flow is then marginally stable, and the stage is set for the expansion. This is the approach followed here.

In strongly dissipative problems this second approach leads to amplitude equations of ordinary differential form for the marginally unstable modes. In the current, almost inviscid problem, this reduction in the dimension of the problem does not occur. The reason is that in dissipative systems, there is a spectral gap between the marginally unstable modes and the other, strongly damped modes in the system, and the usual techniques of centre-manifold theory can be exploited to reduce the dimension (e.g. Guckenheimer & Holmes 1983). For the problem at hand, in which dissipative terms are added perturbatively, the neutral modes lie inside the continuous spectrum of the leading-order, inviscid problem. Hence there is no spectral gap and a dimensional reduction is not possible. What can be achieved will now be explored. The main details of the calculation are presented in Appendix A. Here, the salient features of the expansion will be summarized.

The expansion begins from a marginally stable state, defined by $U = U_0(y)$, which is then perturbed by modifying the background velocity: $U = U_0(y) + \epsilon U_1(y) + \epsilon^2 U_2(y)$. Next, pose the expansions

$$u = \epsilon^2(u_0 + \epsilon u_1 + \cdots), \quad v = \epsilon^2(v_0 + \epsilon v_1 + \cdots) \quad \text{and} \quad h = \epsilon^2(h_0 + \epsilon h_1 + \cdots), \tag{5.1}$$

then transform into a frame moving at the wave speed and rescale time in that frame: $\partial_t \to -U(y_c)\partial_x + \epsilon\partial_T$, where T is a slow timescale on which instability develops, and y_c is the critical level of the neutrally stable mode (an inflection point; $y_c = 0$ for the example quoted earlier). This scaling of the problem ensures that the evolution of the amplitude is controlled by a combination of nonlinearity and viscosity inside the critical layer, and the instability arising through the modification to the marginally stable profile.

The expansions are then substituted into the equations and the system is solved order by order. At leading order, the equations reduce to those for the neutral mode:

$$u_0 = A(T)\hat{u}_0(y)\mathrm{e}^{\mathrm{i}k_m x} + \text{c.c.} \tag{5.2}$$

The amplitude is at this stage undetermined, but at next order, to find a bounded solution, a solvability condition must be applied. This furnishes the evolution equation for the mode amplitude. However, the procedure is complicated because the equations appear to be singular at $y = y_c$. In other words, a critical-level singularity arises.

The apparent singularity is resolved by looking for another solution valid inside a slender region surrounding the critical level, the 'critical layer'. Inside this region, the solution varies on a shorter spatial scale, which is resolved by introducing the stretched coordinate, $Y = y/\epsilon$. Another expansion then furnishes the critical-layer solution that must be matched to the original solution which remains valid outside the critical layer. In other words, one develops expansions in an inner region (the critical layer) and in an outer one (the bulk of the flow), then matches them in an intermediate region in the usual prescription of a matched asymptotic expansion.

The matched asymptotics resolves the apparent singularity and allows the proper formulation of the solvability condition. This results in the evolution equation for A with the novelty that it is coupled to an equation for the potential vorticity inside the critical layer. This is the coupled system

$$I A_T - \mathrm{i}k_m \Omega A = \int_{-\infty}^{\infty}\int_{-\infty}^{\infty} \mathrm{e}^{-\mathrm{i}k_m x}\zeta_x(x, Y, T)\,\mathrm{d}Y\,\mathrm{d}x \tag{5.3}$$

https://doi.org/10.1017/S0022112099004279 Published online by Cambridge University Press

and

$$\partial_T \zeta + Y\zeta_x + \Psi_x \zeta_Y - \nu\zeta_{YY} = \kappa\Psi_T + \gamma\Psi_x, \tag{5.4}$$

where

$$\Psi = A(T)\mathrm{e}^{\mathrm{i}k_m x} + A^*(T)\mathrm{e}^{-\mathrm{i}k_m x}. \tag{5.5}$$

Here $\kappa \propto -U'''(y_c)$ and $\gamma \propto U''(y_c)$, and the coefficients, I and Ω, are defined in Appendix A.

Equations (5.3)–(5.4) are similar to those derived by Goldstein & Hultgren (1988) and Churilov & Shukhman (1987) for incompressible shears, and to the 'single-wave model' of plasma physics, which can be derived from the Vlasov–Poisson equation (del Castillo-Negrete 1998). Presumably, (5.3)–(5.4) constitute a 'normal form' for the amplitude equation describing the bifurcation of an unstable mode from a continuous spectrum. However, there is no rigorous mathematics underlying this result here, unlike in strongly dissipative systems where normal-form theory is well established (Coullet & Spiegel 1983; Guckenheimer & Holmes 1983).

One important feature of the amplitude equations is that the dissipation leads to a slow, viscous spreading of the critical-layer vorticity. Ultimately, this means that the vorticity diffuses out of the region of thickness ϵ and new scalings are needed to describe the long-time solution (Churilov 1989; Goldstein & Hultgren 1988).

5.2. *Reconsidering linear theory*

The linearization of these equations leads to the system

$$IA_T - \mathrm{i}k_m\Omega A = \mathrm{i}k_m \int_{-\infty}^{\infty} \tilde{\zeta}\,\mathrm{d}Y \tag{5.6}$$

and

$$\partial_T \tilde{\zeta} + \mathrm{i}k_m Y\tilde{\zeta} - \nu\tilde{\zeta}_{YY} = \kappa\Psi_T + \mathrm{i}k_m\gamma\Psi, \tag{5.7}$$

on introducing the dependence $\zeta = \tilde{\zeta}(Y,T)\exp \mathrm{i}k_m x$. This set of equations can be solved in closed form for the initial-value problem. Here, though, attention is focused on the normal modes, with dependences $\exp -\mathrm{i}k_m ct$. Then,

$$c_r + \mathrm{i}|c_i| = \frac{I\Omega + \pi^2\kappa\gamma + \mathrm{i}\pi(\kappa\Omega - I\gamma)}{I^2 + \pi^2\kappa^2} \tag{5.8}$$

if $\nu \neq 0$, or

$$c_r + \mathrm{i}c_i = \frac{I\Omega + \pi^2\kappa\gamma + \mathrm{i}\pi(\kappa\Omega - I\gamma)}{I^2 + \pi^2\kappa^2} \tag{5.9}$$

if $\nu = 0$. That is, two dispersion relations that are identical up to the absolute value of c_i that appears in (5.8). This indicates that unstable modes correspond in the two problems when $\kappa\Omega - I\gamma > 0$. But there is only one viscous mode; the decaying inviscid mode has no counterpart (this mode is the consequence of time-reversibility in the inviscid system; Lin 1945). When $\kappa\Omega - I\gamma < 0$, there are no inviscid modes, reflecting the presence of only the continuous spectrum. However, in viscous theory, a mode still exists. This mode corresponds to a peculiar 'quasi-mode' of the inviscid problem. This quasi-mode is an inconsistent solution to (5.8); it has no meaning as a normal mode but, none the less, appears in the initial-value problem (it is a *Landau pole*; Balmforth 1998).

In the example presented in § 3.2, there is a further symmetry that implies that $I = \gamma = 0$. Hence, for this case, $c_r = 0$ and $|c_i| = \Omega/\pi\kappa$ if $\nu = 0$, which is the

https://doi.org/10.1017/S0022112099004279 Published online by Cambridge University Press

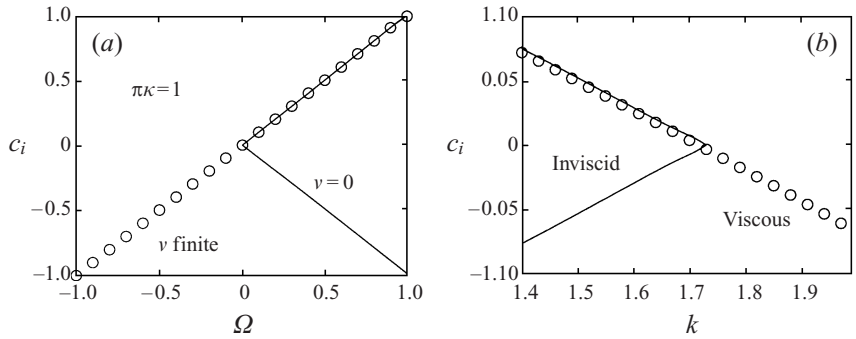


FIGURE 10. Inviscid (solid lines) and viscous (circles) eigenvalues: (*a*) the predictions of the linearized amplitude equations; (*b*) numerically computed eigenvalues for $\epsilon^3 \nu = 10^{-4}$ and the model flow (3.7) with $\alpha = 2$ and $F = 0.25$.

analogue of (4.11), or $c_i = \Omega/\pi\kappa$ if $\nu \neq 0$. The comparison between inviscid and viscous eigenvalues is sketched in figure 10(*a*).

These predictions of the linearized amplitude equations can be directly verified by numerical means. Viscous eigenvalues are furnished by solving the linear equations with the inclusion of the dissipative terms of (2.1)–(2.2). The results of such a calculation are shown in figure 10(*b*), which shows a qualitatively similar picture to the analytical results in panel (*a*). (In the case of the numerical results, the eigenvalues are plotted against k rather than a control parameter of the equilibrium state, but this is not essential.)

6. Low-amplitude, supersonic instability

6.1. *The proliferation of active modes*

The main problem with a weakly nonlinear development of the supersonic instability is that, as noted earlier, whenever there is a band of unstable modes, there are in fact infinitely more such bands, many of which lie in resonant chains. It seems implausible to assume that one may quantize the domain in precisely the correct fashion so as to isolate only a single marginally stable mode. In fact, even were this feasible, there would still be the neutral surface gravity waves that are similarly difficult to ignore.

There are various ways around this difficulty, none of which is particularly satisfying. For example, the instability band at the lowest wavenumbers is typically the most unstable. In the unlikely event that this band was not in resonance with any other modes, neutral or unstable, then one could adopt the Draconian measure of assuming that all the other unstable and neutral modes had zero initial amplitude. This removes them from the nonlinear problem. Alternatively, one can argue that the higher-wavenumber modes are increasingly affected by dissipation (through viscous terms of the form, $-\nu k^2 u$), and so eventually, the resonant chains become very strongly damped and unimportant. Or, if one concentrates only on linear theory (which is, in fact, the main emphasis here), the problematic nonlinear resonances are irrelevant, and one can continue regardless. With these justifications in mind, we press on with the expansion, focusing on the first instability band.

In addition to the proliferation of modes, problems are aggravated still further whenever there are potential vorticity gradients, for then the instability is no longer localized to narrow bands (see figures 6–8). This indicates that the only option for a controlled expansion is to perturb from a state in which the potential vorticity

https://doi.org/10.1017/S0022112099004279 Published online by Cambridge University Press

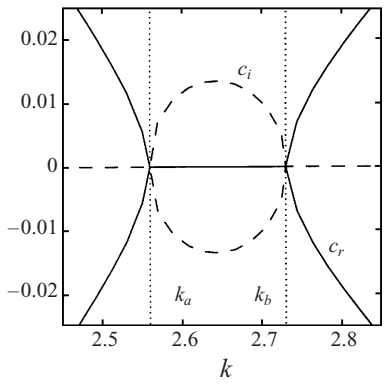


FIGURE 11. The instability band and the neutral stability points.

gradients are zero throughout the shear; that is, Couette flow. Potential vorticity gradients can then be introduced at higher order to gauge their effect.

6.2. *The expansion*

The aim is therefore to consider the weakly nonlinear development of the first instability band for a flow with a weak potential vorticity gradient. The quantization of k is exploited to expand about either of the marginal states bounding the instability band (see figure 11). That is, $k_m = k_a$ or k_b.

It is clear from this picture that at either of the neutral stability points, there are in fact two marginally stable modes. In one direction (in k) they split into a pair of neutral waves, in the other direction into a growing–decaying mode pair. This scenario signifies a degenerate type of bifurcation (a Takens–Bogdanov bifurcation), where complex conjugate modes bifurcate to instability through zero frequency. The most important consequence of this degeneracy is that the equation for the mode amplitude A becomes higher order in time.

It also turns out that, because of the symmetries of the leading-order eigenfunctions at k_a and k_b (see figure 5), the expansion proceeds differently in the two cases. In particular, the expansion at $k = k_a$ is somewhat special, and must be taken to higher order than that at $k = k_b$. The reason for this is that because $v(0) = 0$ for the neutral mode with $k = k_a$, critical-level singularity does not appear until an unusually high order (cf. (3.4)). For simplicity, the analysis specializes to the case $k = k_b$. However, having made this specialization, the amplitude equations that then result apply to much more general situations, including the neutral modes bounding the instability bands with $y_c \neq 0$, and probably even the mode at $k = k_a$ (though this has not been verified).

Again the details of the expansion are relegated to an appendix (Appendix B). Briefly, asymptotic sequences like (5.1) are again posed. At leading order the equations for the neutrally stable mode appear, and the unknown amplitude is denoted by $A(T)$. The evolution equation for A is found on proceeding to higher order. In this case, the expansion must be carried to second order. Here again a solvability condition must be formulated that leads to the evolution equation, but as before there is a critical-level singularity. Once more this signifies the presence of the critical-layer region, and just as for the inflectional instability, the singularity is resolved inside the critical layer. This circumvents the apparent critical-level singularity and again

https://doi.org/10.1017/S0022112099004279 Published online by Cambridge University Press

couples the A-equation to the critical-layer potential vorticity equation:

$$A_{TT} + \mathrm{i}\Omega A_T - \Gamma A = \int_{-\infty}^{\infty}\int_{-\infty}^{\infty} \mathrm{e}^{-\mathrm{i}k_m x}\zeta \,\mathrm{d}x\mathrm{d}Y \tag{6.1}$$

and

$$\zeta_T + Y\zeta_x + \Psi_x\zeta_Y - \nu\zeta_{YY} = \kappa\Psi_T + \gamma\Psi_x, \tag{6.2}$$

with

$$\Psi = A(T)\mathrm{e}^{\mathrm{i}k_m x} + \text{c.c.}, \tag{6.3}$$

where Ω and Γ are convolutions of the linear eigenfunctions and contain the (arbitrary) modifications to the profile, U_1 and U_2, and $\kappa = -\hat{u}'(0)U'''(0)$ and $\gamma = \hat{u}'(0)U''(0)$ where $\hat{u}(y)$ is the neutral mode eigenfunction (shown in figure 5*a*).

6.3. *Linear theory and effects of weak viscosity*

On dropping the nonlinear terms and taking the dependence, $\zeta = \tilde{\zeta}(Y, T)\mathrm{e}^{\mathrm{i}k_m x}$, one finds

$$A_{TT} + \mathrm{i}\Omega A_T - \Gamma A = \int_{-\infty}^{\infty} \tilde{\zeta}\,\mathrm{d}Y \tag{6.4}$$

and

$$\tilde{\zeta}_T + \mathrm{i}k_m Y\tilde{\zeta} - \nu\tilde{\zeta}_{YY} = \kappa A_T + \mathrm{i}k_m\gamma A. \tag{6.5}$$

The normal-mode dispersion relation then follows as

$$\Gamma - \Omega k_m c + k_m^2 c^2 = \mathrm{i}\pi(\kappa c - \gamma)s, \tag{6.6}$$

where

$$s = \begin{cases} \mathrm{sgn}(c_i) & \text{if } \nu = 0 \\ 1 & \text{if } \nu \neq 0. \end{cases} \tag{6.7}$$

This is the general dispersion relation for modes bordering an instability band in the presence of potential vorticity gradients.

In the special case for which $U(y)$ is antisymmetrical, then, as noted in Appendix B, $\Omega = \gamma = 0$. Hence, the dispersion relation reduces to

$$\Gamma + k_m^2 c^2 = \mathrm{i}\pi\kappa c s. \tag{6.8}$$

This gives either

$$\text{(outside)} \quad c_r = \pm\frac{1}{2k_m^2}(-4k_m^2\Gamma - \pi^2\kappa^2)^{1/2}, \quad sc_i = \frac{\pi\kappa}{2k_m^2}, \quad \text{if } \Gamma < -\pi^2\kappa^2/4k_m^2, \tag{6.9}$$

or

$$\text{(inside)} \quad c_r = 0, \quad sc_i = \frac{\pi\kappa \pm (\pi^2\kappa^2 + 4k_m^2\Gamma)^{1/2}}{2k_m^2}, \quad \text{if } \Gamma > -\pi^2\kappa^2/4k_m^2. \tag{6.10}$$

As indicated by the labels, the first of these relations corresponds to values of Γ for which k_m is shifted away from the instability band; the second describes the situation when k_m is moved inside the band.

The solutions to the dispersion relations (6.9)–(6.10) are illustrated in figure 12. Note that viscosity does not lead to a damping term in the linear theory of the amplitude equations. It does, however, affect the structure of the eigenvalues.

If $\kappa = 0$, the instability bands of the constant potential vorticity case are recovered:

$$\text{(outside)} \quad c_r = \pm\frac{1}{k_m}(-\Gamma)^{1/2}, \quad c_i = 0, \quad \text{if } \Gamma < 0, \tag{6.11}$$

https://doi.org/10.1017/S0022112099004279 Published online by Cambridge University Press

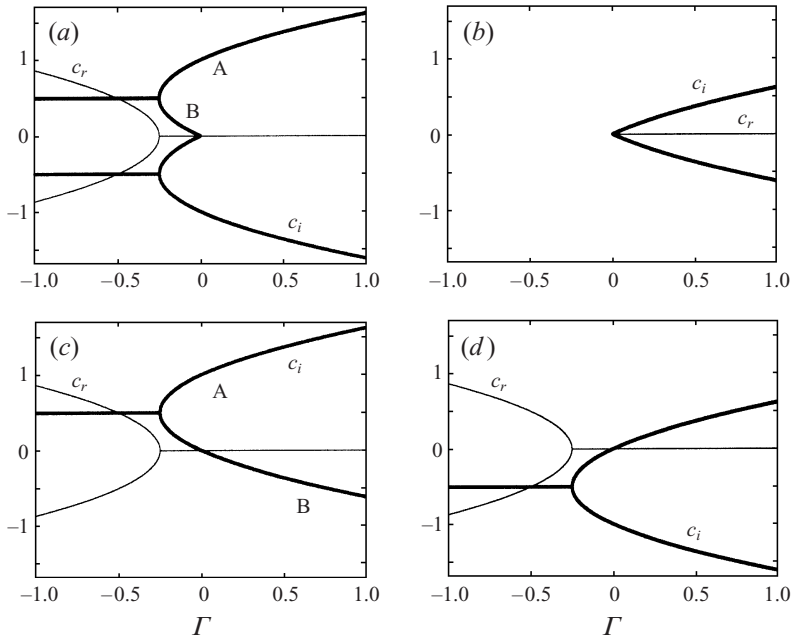


FIGURE 12. Solutions to the dispersion relation (6.9)–(6.10) for (*a*) $v = 0$, $\pi\kappa = 1$ and $k_m = 1$, (*b*) $v = 0$, $\pi\kappa = -1$ and $k_m = 1$, (*c*) $v \neq 0$, $\pi\kappa = 1$ and $k_m = 1$ and (*d*) $v \neq 0$, $\pi\kappa = -1$ and $k_m = 1$.

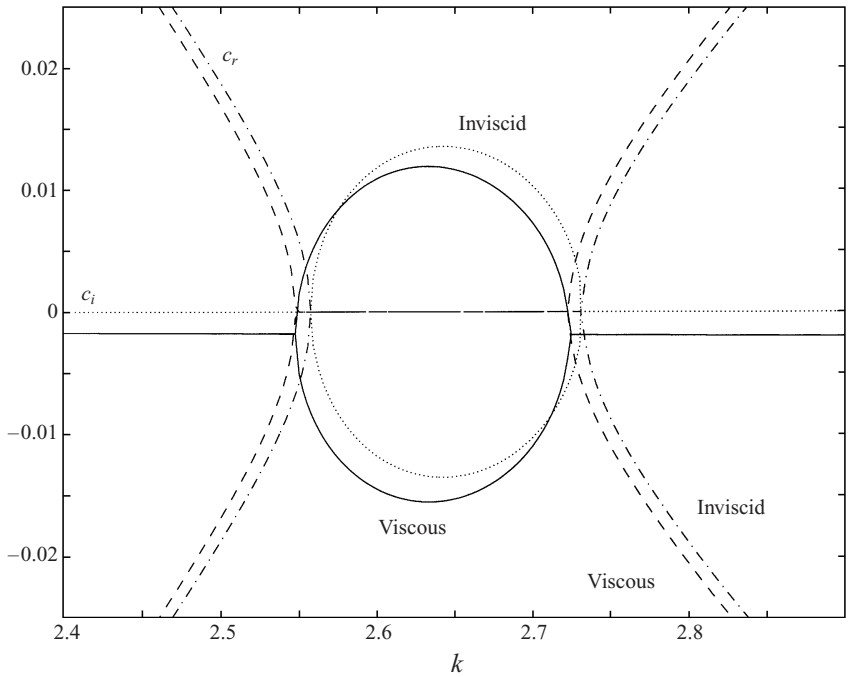


FIGURE 13. Numerically computed eigenvalues for the lowest-wavenumber instability band in Couette flow ($F = 2$, $\alpha = 0$). The solid and dashed lines show the viscous eigenvalues, and the dotted and dashed-dotted lines indicate the inviscid values. The viscous coefficient $\epsilon^3 v = 10^{-4}$ (that is, the Reynolds number is 10^4).

https://doi.org/10.1017/S0022112099004279 Published online by Cambridge University Press

or

$$\text{(inside)} \quad c_r = 0, \quad c_i = \pm\frac{1}{k_m}\Gamma^{1/2}, \quad \text{if } \Gamma > 0. \tag{6.12}$$

The eigenvalues in (6.11)–(6.12) are valid for both $v = 0$ and $v \neq 0$, and so viscosity has no effect on the modal structure in this particular case. This is also seen in figure 13, which compares numerically computed viscous and inviscid eigenvalues (obtained by solving the linear equations with the viscous terms of (2.1)–(2.2) retained). Related results are given by Glatzel (1989).

When $\kappa \neq 0$, the criterion for entering the instability band becomes $\Gamma > -\pi^2\kappa^2/4k_m^2$. Thus, in most cases, the band is broadened by the effect of finite potential vorticity gradients (as indicated in figure 12*b*, this is not true if $v = 0$ and $\kappa < 0$). This effect is seen in the numerical solutions displayed in figures 4–7. In addition, the modal structure is very different in the inviscid and viscous cases.

For $v = 0$ and $\kappa < 0$, then (6.9)–(6.10) imply that there are no modes in $\Gamma < 0$ (see figure 12*b*). Equivalently, over this region, there are quasi-modes (the inconsistent solutions to (6.9)–(6.10)). When $\kappa > 0$, on the other hand, there is a growing–decaying pair in $\Gamma < -\pi^2\kappa^2/4k_m^2$ (figure 12*a*). This is a repetition of the earlier result obtained from (4.11): outside the instability bands, modes either disappear or become unstable-decaying mode pairs on the introduction of a finite potential vorticity gradient.

The inviscid modes that lie inside the instability band for $\kappa = 0$ continue to exist when $\kappa \neq 0$. In the dispersion relations this arises because there is always one of the solutions in (6.10) that is permitted by the absolute value. In other words, the finite potential vorticity gradient does not destroy the instability band. However, there are two bifurcations possible: when $\kappa < 0$, modes appear out of the continuous spectrum (figure 12*b*), and if $\kappa > 0$, growing–decaying modes continue into the band as shown in figure 12(*a*).

These predictions can be compared with the numerical results presented in § 4. The eigenvalues that enter the instability band in figure 6 at $k \approx 2.4$ correspond to the modes denoted 'A' in figure 12(*a*); those that appear at $k \approx 2.3$ in figure 8 parallel the emergence of the pair in figure 12(*b*). Note that if $\kappa > 0$ there is another unstable-decaying mode pair for $-\pi^2\kappa^2/4k_m^2 < \Gamma < 0$. These modes are the solutions from the $-$ sign in (6.10), and are labelled B in figure 12(*a*). These other modes were not detected in the numerical calculations.

The $\kappa \neq 0$ solutions are somewhat different with viscosity ($v \neq 0$; $s \equiv 1$). Now there are no absolute values in (6.9)–(6.10). This means that there is no disappearance of modes in regions with the 'wrong' sign of κ; instead there are true, decaying modes (compare panels *b* and *d* in figure 12). Moreover, of the two solutions inside the instability band, one (labelled A in figure 12*c*) is analogous to the inviscid instability. The other (labelled B in figure 12*c*) is decaying, but is not the same as the decaying inviscid mode in this region; in fact, it corresponds to a quasi-mode. In other words, once again, the inviscid decaying mode disappears on introducing viscosity (Lin 1945), and the damped viscous modes correspond to quasi-modes. These features parallel what happens on adding viscosity to the inflectional instability (§ 5) and in the incompressible shear-flow problem (Balmforth 1998).

Some numerical results are displayed in figures 14 and 15; these agree with the predictions shown in figure 12(*c*, *d*). Figures 14 and 15 show viscous eigenvalues for the two lowest-order surface gravity waves of the model (3.7) with $\alpha = 0.5$ and $F = 2$ (so figure 14 is analogous to figure 6), and of the flow with $U(y) = (y + 0.1y^3)/1.1$ (compare figure 15 to figure 8). There are four modes for each k in these pictures,

https://doi.org/10.1017/S0022112099004279 Published online by Cambridge University Press

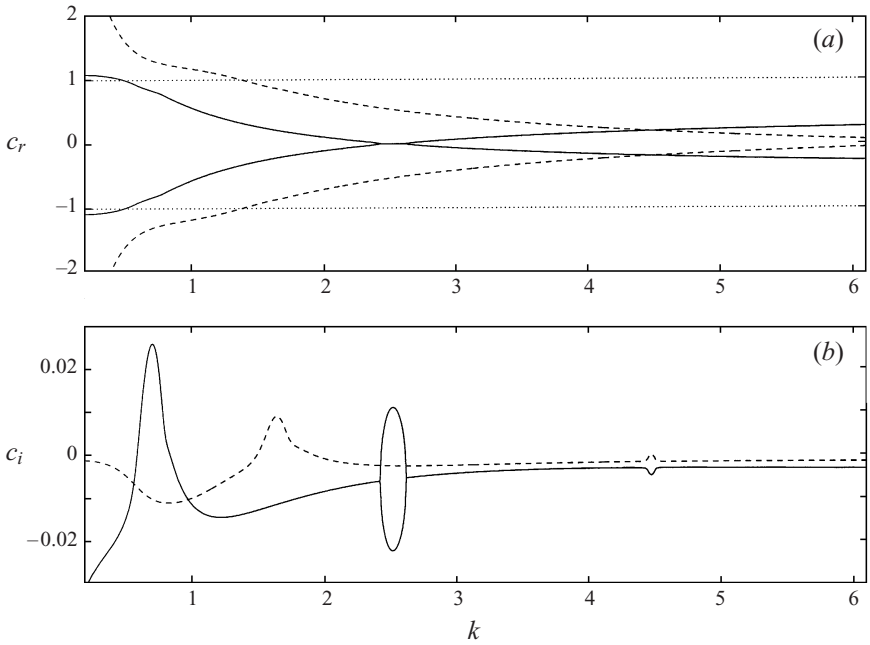


FIGURE 14. Numerically computed viscous eigenvalues for the model flow (3.7) with $\alpha = 0.5$ and $F = 2$. This picture shows the viscous analogue of figure 6. The viscous coefficient is given by $\epsilon^3 \nu = 10^{-4}$ (that is, the Reynolds number is 10^4).

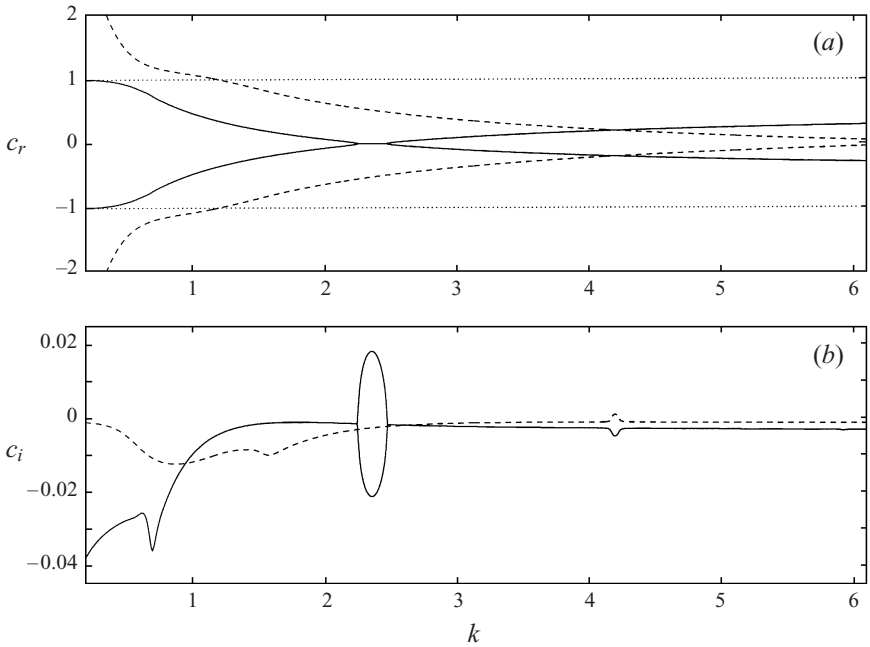


FIGURE 15. Numerically computed viscous eigenvalues for $U(y) = (y + 0.1y^3)/1.1$ and $F = 2$. This picture shows the viscous analogue of figure 8. The viscous coefficient is given by $\epsilon^3 \nu = 10^{-4}$ (that is, the Reynolds number is 10^4).

https://doi.org/10.1017/S0022112099004279 Published online by Cambridge University Press

unlike in the inviscid versions. Away from the instability band at $c_r = 0$, the modes are the viscous analogues of either unstable inviscid modes or quasi-modes (for example, in figure 14, the mode pair shown by solid lines for $k < 2.4$ corresponds to an inviscid instability, and for $k > 2.65$ they correspond to a pair of quasi-modes). Note that viscosity has a destabilizing effect over some ranges of k for the tanh profile (the peak in growth rates at $k \approx 0.7$ and $k \approx 1.6$ in figure 14 are noticeably higher than in the inviscid case), but not for the cubic profile, and that the structure of the secondary instability bands at $k \approx 4.5$ in figure 14 and $k \approx 4.2$ in figure 15 can also be understood using equation (6.6).

7. Conclusions

In this paper, the linear stability problem for shear flow in shallow water has been solved numerically. Instabilities have been classified into two catagories, inflectional and supersonic. In the examples presented here, this classification is unambiguous: the inflectional instability can be continued to the incompressible limit where it becomes analogous to Rayleigh's instability, and the supersonic instabilities can be traced to the surface gravity waves of the shallow water Couette problem. Moreover, the two types of instabilities reside in different regions of parameter space. However, the distinction may well become ambiguous for general profiles.

Some analytical arguments based on conservation laws and short-wavelength theory have been used to clarify the results. Notably, the effects of finite potential vorticity gradients have been elucidated. Then, critical-layer expansions were employed to construct theories for the evolution of marginally stable modes. This theory was used to reconsider the linear problem and give reduced dispersion relations of closed form. Moreover, the theory reveals the effect of weak viscosity.

The analysis of the evolution equations could be taken much further. The reduced formulation of the problem facilitates a straightforward discussion of effects such as transient amplification (the Orr mechanism, Farrell 1982). One notable feature of the shallow water problem that is evident from the amplitude equations is that this mechanism can amplify the surface gravity waves as well as vortical disturbances (the vorticity inside the critical layer provides a source term in the amplitude equation (6.4)). Nonlinear theory can also be developed. For example, nonlinear equilibrium states can be constructed relatively simply (Balmforth & Young 1997; del Castillo-Negrete 1998). For the supersonic instabilities, these equilibrium states are finite-amplitude surface gravity waves with cat's-eye patterns centred at the critical level.

However, the weakly nonlinear theory for inflectional instability is little different to that for incompressible fluid shears and so there is less novelty in proceeding down that pathway. Theory of the supersonic instability, however, is higher-order in time, and presumably contains more physics than the inflectional version. It might, therefore, be worthwhile to pursue that version of the theory. But this is left for future work.

The main failing of the perturbation expansions is that in the over-reflectional case, there is no proper justification for isolating a single neutral mode and exploring its weakly nonlinear development in isolation of the other modes of the system. This is because as soon as there is instability, there are infinitely many instability bands that often lie at commensurate wavenumbers. The situation is further aggravated by finite potential vorticity gradients that substantially extend the range of unstable wavenumbers. This makes weakly nonlinear theory extraordinarily difficult without some sort of Draconian measure like the one adopted here.

https://doi.org/10.1017/S0022112099004279 Published online by Cambridge University Press

I thank the Green Foundation (IGPP, UCSD) for support and the Nuffield foundation for an equipment grant. This work was also partly supported by the National Science Foundation Award OCE 9529824. I appreciate conversations with W. R. Young and E. A. Spiegel.

Appendix A. Inflectional instability

A.1. *Outer solution*

As pointed out earlier, the marginally unstable mode with $k = k_c = k_m$ has a critical level lying at the inflection point of the profile, $y_c = c = 0$. This solution provides the leading-order solution about which the weakly nonlinear expansion develops.

To perturb the system and edge it into the nonlinear regime two options are open. The domain size may be increased slightly beyond the marginal value, so that $k_m < k_c$. Alternatively, the equilibrium profiles $U(y)$ and $H(y)$ could be modified slightly. Here, the domain size is fixed at the marginal value and a slight distortion introduced into the model flow profile:

$$U(y) = U_0(y) + \epsilon U_1(y), \tag{A 1}$$

where $U_0(y)$ is, for example, the tanh profile, and $\epsilon U_1(y)$ is the distortion, which does not necessarily preserve the location of the inflection point; that is, $U_1''(0) \neq 0$. The simplification $U_1(0) = 0$ is taken, which is neither necessary nor important (if $U_1(0) \neq 0$, then the critical level is shifted at order ϵ, but this is easily accounted for). The amplitude ϵ is the small parameter that is used to order the expansion.

Since the marginal mode is stationary, the time development of any instability is slow and so the first step in the asymptotic calculation is to rescale time and introduce a long time coordinate, $T = \epsilon t$ (if the wave speed of the marginally unstable mode is finite, two timescales are needed; the faster timescale simply corresponds to the shift needed to move into a frame travelling with the wave speed).

Next, introduce the series,

$$u = \epsilon^2(u_0 + \epsilon u_1 + \cdots), \quad v = \epsilon^2(v_0 + \epsilon v_1 + \cdots), \quad h = \epsilon^2(h_0 + \epsilon h_1 + \cdots) \tag{A 2}$$

and

$$q = \epsilon^2(q_0 + \epsilon q_1 + \cdots), \tag{A 3}$$

into the governing equations. Terms of like order in ϵ are then grouped together to generate an asymptotic hierarcy of equations.

The various scalings in (A 1)–(A 3), together with $T = \epsilon t$ and the scaling of the viscous terms in (2.1)–(2.3) comprise a distinguished scaling of the effects of viscosity, nonlinearity, and the degree of instability. This choice is made to bring all these effects into the amplitude equation at the same order of ϵ. From a physical perspective, the scalings focus attention on the slow growth of the marginally unstable mode, with a growth rate determined by the modification to the basic state, and this is controlled by nonlinearity and viscosity inside the critical layer. The specialization to slow evolution eliminates the relatively fast surface gravity waves from the expansion.

At leading order, h_0 may be eliminated from the equations and the system may be written in the form

$$q_0 - \frac{U_0''}{U_0}\psi_0 = 0 \tag{A 4}$$

and

$$\psi_0' - \tfrac{1}{2}F^2(U_0^2)'\psi_0 + (1 - F^2U_0^2)u_0 = 0, \tag{A 5}$$

https://doi.org/10.1017/S0022112099004279 Published online by Cambridge University Press

with

$$q_0 = -u_0' - \tfrac{1}{2}F^2(U_0^2)'u_0 + [k_m^2 + F^2(U_0')^2]\psi_0, \tag{A 6}$$

where $v = \psi_x$ defines a potential somewhat like a streamfunction. This system is of the form

$$\mathscr{L}\begin{pmatrix} u_0 \\ \psi_0 \end{pmatrix} = \begin{pmatrix} 0 \\ 0 \end{pmatrix}, \tag{A 7}$$

with $\mathscr{L}$ a particular differential operator. The solution is written

$$\begin{pmatrix} u_0 \\ \psi_0 \end{pmatrix} = A(T)\begin{pmatrix} \hat{u}_0 \\ \hat{\psi}_0 \end{pmatrix} + \text{c.c.}, \tag{A 8}$$

where the amplitude $A(T)$ is at this stage undetermined. This solution is displayed for the example profile of the main text in figure 2. Note that the adjoint to the system (A 7) is the vector $(\hat{\psi}_0, -\hat{u}_0)$, once an inner product is defined as the usual scalar product integrated over y.

At order ϵ^2, the system of equations is

$$U_0 u_{1x} + U_0' v_1 + \frac{1}{F^2}h_{1x} = -(\partial_T + U_1\partial_x)\,u_0 - U_1' v_0, \tag{A 9}$$

$$U_0 v_{1x} + \frac{1}{F^2}h_{1y} = -(\partial_T + U_1\partial_x)v_0 \tag{A 10}$$

and

$$U_0 h_{1x} + u_{1x} + v_{1y} = -(\partial_T + U_1\partial_x)h_0. \tag{A 11}$$

These equations can be manipulated into the relations,

$$q_1 - \frac{U_0''}{U_0}\psi_1 = -\left(\frac{\partial_T}{\mathrm{i}k_m} + U_1\right)\frac{U_0''\psi_0}{U_0^2} + \frac{U_1''\psi_0}{U_0} \tag{A 12}$$

and

$$\psi_{1y} - \tfrac{1}{2}F^2(U_0^2)'\psi_1 + (1 - F^2U_0^2)u_1 = F^2\left(\frac{\partial_T}{\mathrm{i}k_m} + U_1\right)(U_0'\psi_0 + U_0u_0) + F^2U_0U_1'\psi_0, \tag{A 13}$$

with

$$\begin{aligned} q_1 = {} & -u_{1y} - \tfrac{1}{2}F^2(U_0^2)'u_1 + [k_m^2 + F^2(U_0')^2]\psi_1 \\ & + F^2U_0'\left[\left(\frac{\partial_T}{\mathrm{i}k_m} + U_1\right)u_0 + 2U_1'\psi_0\right] + F^2U_0U_1'u_0. \end{aligned} \tag{A 14}$$

This set of equations is of the form

$$\mathscr{L}\begin{pmatrix} u_1 \\ \psi_1 \end{pmatrix} = \begin{pmatrix} N_1 \\ N_2 \end{pmatrix}, \tag{A 15}$$

for some N_1 and N_2. Under normal circumstances one would now take an inner product with the adjoint, the left-hand side then disappears leaving a solvability condition on the leading-order solution that is tantamount to determining A. However, in the present problem this Fredholm alternative cannot immediately be taken; the right-hand side of (A 12) is singular as $y \to 0$.

In fact, it is straightforward to observe that the leading-order solution has the dependence

$$\psi_0 = O(1), \quad u_0 = O(y) \quad \text{and} \quad q_0 = O(1) \quad \text{as } y \to 0, \tag{A 16}$$

https://doi.org/10.1017/S0022112099004279 Published online by Cambridge University Press

whilst $q_1 = O(y^{-1})$. Thus terms break order when $y \to O(\epsilon)$. This signifies the presence of a slender region around the critical level, the critical layer, inside which the asymptotic solution described above breaks down and the equations must be rescaled to look for another solution.

A.2. *Inner solution*

For the critical layer, introduce the inner coordinate, $Y = y/\epsilon$. Also, set $h = \epsilon^2 h_I$ and $v = \epsilon^2 v_I$. Then, only the leading-order terms of the cross-stream momentum equation (2.2) and the continuity equation (2.3) are of interest. These imply

$$h_{IY} = v_{IY} = 0. \tag{A 17}$$

The streamwise momentum equation (2.1) indicates that

$$U'_{0c} v_I + \frac{1}{F^2} h_{Ix} = 0, \tag{A 18}$$

where the subscript c signifies the value of the quantity at the critical level, $y = 0$. Equivalently, $h_I = -F^2 U'_{0c} \Psi$, if $\Psi_x = v_I$.

The definition of potential vorticity inside the critical layer gives the relation

$$q = \epsilon^2 q_I = -\frac{1}{\epsilon} u_Y + \epsilon^2 (v_{Ix} + U'_{0c} h_I) + O(\epsilon^3). \tag{A 19}$$

Thus u must be order ϵ^3 inside the critical layer, which is consistent with the limiting behaviour of the leading-order outer solution in (A 16). On setting $u = \epsilon^3 u_I$, (A 19) becomes

$$u_{IY} = -q_I + v_{Ix} + U'_{0c} h_I \equiv -q_I + \Psi_{xx} - F^2 U'_{0c} \Psi. \tag{A 20}$$

Finally, the potential vorticity equation is, to leading order,

$$\partial_T q_I + U'_{0c} Y q_{Ix} + \Psi_x q_{IY} - \nu q_{IYY} = U'''_{0c} Y \Psi_x + U''_{1c} \Psi_x. \tag{A 21}$$

This equation implies that the limiting behaviour of q_I as $|Y| \to \infty$ is

$$q_I \sim \frac{U'''_{0c}}{U'_{0c}} \Psi. \tag{A 22}$$

It is convenient to subtract this asymptotic value from the inner potential vorticity variable. Hence introduce the local potential vorticity of the critical layer region,

$$\zeta = q_I - \frac{U'''_{0c}}{U'_{0c}} \Psi. \tag{A 23}$$

In terms of the new variable, the potential vorticity equation is

$$\partial_T \zeta + U'_{0c} Y \zeta_x + \Psi_x \zeta_Y - \nu \zeta_{YY} = -\frac{U'''_{0c}}{U'_{0c}} \Psi_T + U''_{1c} \Psi_x. \tag{A 24}$$

The asymptotic behaviour of the new variable is

$$\zeta_x \sim -\frac{U'''_{0c}}{U'^2_{0c} Y} \Psi_T + \frac{U''_{1c}}{U'_{0c} Y} \Psi_x. \tag{A 25}$$

Hence ζ is localized within the critical layer.

A.3. *Matching*

The inner and outer solutions are matched by taking the variables in turn. Since v_I and h_I are, to leading order, independent of Y inside the critical layer, these variables

https://doi.org/10.1017/S0022112099004279 Published online by Cambridge University Press

may be taken to be simply the limit of the outer solution. In particular, a match with the outer solution is achieved on taking $\Psi = A\hat{\psi}_0(0)$. Similarly, the potential vorticity is matched relatively simply: the outer limits of the inner solution revealed in (A 22) and (A 25) are what is required to match the outer solution, $\epsilon^2(q_0 + \epsilon q_1)$, as $y \to 0$.

The only variable requiring more consideration is the streamwise velocity u. Equation (A 20) indicates that the inner solution has the form $u \sim \epsilon^3 u_I$, with

$$u_I(Y) - u_I(0) = -\int_0^Y \left[q_I(x, Y', T) - \frac{U_{0c}'''}{U_{0c}'}\Psi\right] \mathrm{d}Y' - \left(\Psi_{xx} - F^2 U_{0c}'\Psi + \frac{U_{0c}'''}{U_{0c}'}\Psi\right) Y. \tag{A 26}$$

The outer solution, on the other hand, takes the form

$$u \sim \epsilon^3 \left(u_1 + u_{0c} y/\epsilon\right) \quad \text{as } y \to 0^{\pm} \tag{A 27}$$

$$\equiv \epsilon^3 \left[u_1 - \left(\psi_{0cxx} - F^2 U_{0c}'^2 \psi_{0c} + \frac{U_{0c}'''}{U_{0c}'}\psi_{0c}\right)\frac{y}{\epsilon}\right]. \tag{A 28}$$

The quantities in (A 27) and (A 28) must be matched in an intermediate region in which $y \to 0$ and $Y \to \infty$. Let $Y = 1/\varepsilon$ and $y = \epsilon/\varepsilon$ with $\varepsilon \to 0$ and $1 \gg \varepsilon \gg \epsilon$. Thence,

$$[u_1]_{-\varepsilon}^{\varepsilon} = -\int_{-\varepsilon/\epsilon}^{\varepsilon/\epsilon} \zeta(x, Y, T)\mathrm{d}Y. \tag{A 29}$$

Or,

$$u_1(x, 0^+, T) - u_1(x, 0^-, T) = -\int_{-\infty}^{\infty} \zeta(x, Y, T)\mathrm{d}Y, \tag{A 30}$$

in the limit $\varepsilon \to 0$. Note that, because of the far-field behaviour in (A 25) the limits of the integral must be interpreted in terms of a principal value.

Strictly speaking, this matching is not quite compatible with a formal asymptotic expansion: the outer solution u_1, through (A 12) and (A 14), contains a term proportional to $\log|y|$, and the inner solution, through (A 20) and (A 25), a term given by $\log|Y|$. This indicates that the expansion should really contain additional terms of order $\epsilon^2 \log\epsilon$ and higher (cf. Stewartson 1978; Warn & Warn 1978). These terms show up as apparent divergences in the inner limit of the outer solution, and the outer limit of the inner solution. Here, these divergences are dealt with using principal values. However, they may be explicitly taken into account in a modified expansion. Once the solutions u_1 and u_I are further divided into a series in $\epsilon\log\epsilon$, the logarithmic terms are isolated and match automatically as a result of higher-order matchings. However, with the principal value interpretations, this subtlety of the problem need not be considered further.

A.4. *Solvability*

The solvability condition needed to find the equation for A can now be applied by multiplying (A 12) by $\hat{\psi}_1$, (A 13) by $\hat{u}_1$, integrating over y and then subtracting the two equations. To avoid the singularity of (A 12) at $y = 0$, the integral is broken into two pieces over the intervals $[-1, -\varepsilon]$ and $[\varepsilon, 1]$, with $\varepsilon \to 0$ (as in one definition of the Cauchy principal value). The usual manipulations can then be used to eliminate the second-order variables ψ_2 and u_2. However, this cannot be done completely because the integration by parts in the integrated version of (A 12) leaves a term involving the jump in the second-order streamwise velocity, u_2, across the critical layer; that is, the quantity in (A 30) (or at least that part proportional to $\mathrm{e}^{\mathrm{i}k_m x}$). But this connects the

https://doi.org/10.1017/S0022112099004279 Published online by Cambridge University Press

amplitude of the marginally unstable mode to the evolving potential vorticity field inside the critical layer.

The outcome of the manipulations is the equation,

$$I A_T - \mathrm{i}k_m \Omega A = \hat{\psi}_{0c} \int_{-\infty}^{\infty} \int_{-\infty}^{\infty} \mathrm{e}^{-\mathrm{i}k_m x} \zeta_x(x, Y, T) \mathrm{d}Y \, \mathrm{d}x, \tag{A 31}$$

where

$$\Omega = \mathscr{P} \int_{-1}^{1} \left[\left(\frac{U_1 U_0''}{U_0^2} + \frac{U_1''}{U_0} \right) \hat{\psi}_0^2 + F^2 U_1 \left(2U_0' \hat{\psi}_0 + U_0 \hat{u}_0 \right) \hat{u}_0 \right. \tag{A 32}$$

$$\left. + 2F^2 U_1' \left(U_0' \hat{\psi}_0 + U_0 \hat{u}_0 \right) \hat{\psi}_0 \right] \mathrm{d}y, \tag{A 33}$$

and

$$I = \mathscr{P} \int_{-1}^{1} \left[\frac{U_0''}{U_0^2} \hat{\psi}_0^2 + F^2 \left(2U_0' \hat{\psi}_0 + U_0 \hat{u}_0 \right) \hat{u}_0 \right] \mathrm{d}y. \tag{A 34}$$

The symbol $\mathscr{P}$ denotes Cauchy principal value. Together with the inner potential vorticity equation (A 24), this relation completes the system governing the evolution of the marginal mode. This is a partial differential equation coupled to an ordinary differential equation, that is, another infinite-dimensional problem.

With suitable rescaling of Y and A, the choice $\hat{\psi}_{0c} = 1$ and a redefinition of v, the system can be placed into the form quoted in the main text for $\kappa = -U_{0c}'''/(U_{0c}')^2$ and $\gamma = U_{1c}''/U_{0c}'$.

Appendix B. Supersonic instability

This Appendix derives equations for the slow development of marginally unstable modes located at the right-hand edge of the lowest-wavenumber instability band. To begin, introduce the following:

$$\partial_t \to \epsilon \partial_T, \quad U = y + \epsilon U_1(y) + \epsilon^2 U_2(y), \quad F^2 = F_0^2 + \epsilon f_1, \tag{B 1}$$

$$u = \epsilon^2 \tilde{u}, \quad v = \epsilon^2 \tilde{v}, \quad h = \epsilon^2 \tilde{h}. \tag{B 2}$$

A variation in the Froude number is included in (B 1) for reasons that will become evident. Then, on dropping the tildes, the governing equations take the form

$$y u_x + v + \frac{1}{F_0^2} h_x = -\epsilon u_T + \frac{\epsilon f_1 h_x}{F_0^2 (F_0^2 + \epsilon f_1)}$$

$$- \epsilon U_1 u_x - \epsilon U_1' v - \epsilon^2 U_2 u_x - \epsilon^2 U_2' v - \epsilon^2 u u_x - \epsilon^2 v u_y + \epsilon^3 \nu (u_{xx} + u_{yy}), \tag{B 3}$$

$$y v_x + \frac{1}{F_0^2} h_y = -\epsilon u_T + \frac{\epsilon f_1 h_y}{F_0^2 (F_0^2 + \epsilon f_1)} - \epsilon U_1 v_x - \epsilon^2 U_2 v_x - \epsilon^2 u v_x - \epsilon^2 v v_y + \epsilon^3 \nu (v_{xx} + v_{yy}) \tag{B 4}$$

and

$$y h_x + u_x + v_y = -\epsilon h_T - \epsilon U_1 h_x - \epsilon^2 U_2 h_x - \epsilon^2 (hu)_x - \epsilon^2 (hv)_y, \tag{B 5}$$

to the highest, interesting orders in ϵ (note that the viscous terms have now been replaced by the simpler, Laplacian form).

Now pose the asymptotic sequences

$$u = u_0 + \epsilon^1 u_1 + \epsilon^2 u_2 + \cdots, \quad v = v_0 + \epsilon^1 v_1 + \epsilon^2 v_2 + \cdots, \quad h = h_0 + \epsilon^1 h_1 + \epsilon^2 h_2 + \cdots \tag{B 6}$$

and solve order by order.

https://doi.org/10.1017/S0022112099004279 Published online by Cambridge University Press

As a final prelude, some simplifications are introduced if

$$U_1(0) = U_2(0) = U_1'(0) = U_2'(0) = 0 \tag{B 7}$$

and

$$U_1''(0) = 0, \quad U_1'''(0) \neq 0 \quad \text{and} \quad U_2''(0) \neq 0. \tag{B 8}$$

The first two of the relations in (B 7) indicate that the critical level is not shifted on modifying the profile; without the second two, the critical-layer coordinate Y would need rescaling at some stage. These simplifications are not strictly necessary and do not affect the important terms in the weakly nonlinear theory. The conditions in (B 8) indicate that the potential vorticity gradient is order ϵ^2 at the critical level and agree with the form suggested by the small-α expansion of (3.7).

B.1. *Order one*

$$yu_{0x} + v_0 + \frac{1}{F_0^2} h_{0x} = 0, \tag{B 9}$$

$$yv_{0x} + \frac{1}{F_0^2} h_{0y} = 0 \tag{B 10}$$

and

$$yh_{0x} + u_{0x} + v_{0y} = 0. \tag{B 11}$$

On taking the dependence, $\exp(\mathrm{i}k_m x)$, these may be combined into the single equation

$$u_{0yy} - k_m^2(1 - F_0^2 y^2)u_0 = 0. \tag{B 12}$$

The solution is written formally as

$$u_0 = \hat{u}_0(y)A(T) + \text{c.c.}, \tag{B 13}$$

with $A(T)$ the currently undetermined amplitude, and is illustrated in figure 5(*a*).

B.2. *Order* ϵ

$$yu_{1x} + v_1 + \frac{1}{F_0^2} h_{1x} = -u_{0T} - U_1 u_{0x} - U_1' v_0 + \frac{f_1}{F_0^4} h_{0x}, \tag{B 14}$$

$$yv_{1x} + \frac{1}{F_0^2} h_{1y} = -v_{0T} - U_1 v_{0x} + \frac{f_1}{F_0^4} h_{0y} \tag{B 15}$$

and

$$yh_{1x} + u_{1x} + v_{1y} = -h_{0T} - U_1 h_{0x}. \tag{B 16}$$

These equations combine into the potential vorticity relation,

$$-y(u_{1y} - v_{1x} - h_1 - U_1' h_0)_x \equiv yq_{1x} = U_1'' v_0. \tag{B 17}$$

Thus $q_1 = U_1'' \psi_0 / y$, where $\psi_x = v$, which is finite at $y = 0$ through (B 8).

Again, on taking the dependence $\exp(\mathrm{i}k_m x)$, these may be combined into a single equation,

$$\mathscr{L}u_1 = 2\mathrm{i}k_m F_0^2 y(u_{0T} + \mathrm{i}k_m U_1 u_0) - k_m^2 f_1 y^2 u_0 - \frac{1}{y} U_1''' \psi_0 - \frac{1}{y^2} U_1''(yu_0 - \psi_0), \tag{B 18}$$

where $\mathscr{L}$ is the self-adjoint operator defined by

$$\mathscr{L}u = u_{yy} - k_m^2(1 - F_0^2 y^2)u. \tag{B 19}$$

https://doi.org/10.1017/S0022112099004279 Published online by Cambridge University Press

Note that, despite the appearance of the right-hand side of (B 18), there is no critical-level singularity at this order (the apparently divergent terms on the right of (B 18) arise from q_{1y} which is regular).

Equation (B 19) does not, for general f_1 and U_1, have a bounded solution. In fact, this is why f_1 was introduced. The modification to the profile, $U_1(y)$, changes the position of the instability band at order ϵ. Hence, in principle, a perturbation to the wavenumber k_m is needed in order to account for this. However, by suitably modifying the Froude number the shift in the instability band can be countered and the modification to k_m avoided. Thus, in (B 18) a solvability condition is taken (obtained on multiplying by $\hat{u}_0$ and integrating) that fixes f_1; this is equivalent to preserving the location of the instability band:

$$f_1 k_m^2 \int_{-1}^{1} y^2 \hat{u}_0^2 \mathrm{d}y = \int_{-1}^{1} \left[\frac{1}{y^2} U_1''(\hat{\psi}_0 - y\hat{u}_0) - 2k_m^2 F_0^2 y U_1 \hat{u}_0 - \frac{1}{y} U_1''' \hat{\psi}_0 \right] \hat{u}_0 \mathrm{d}y, \qquad \text{(B 20)}$$

where $\psi_0 = A\hat{\psi}_0$. Note that the first term on the right-hand side of (B 18) does not appear in the solvability condition because $yu_{0T}\hat{u}_0 \equiv y\hat{u}_0^2 A_T$, which integrates to zero. This reflects the degeneracy of the normal-mode problem at the neutral stability point.

Once f_1 is selected according to (B 20) and solvability satisfied, the relevant solution to (B 18) is written in the form

$$u_1 = \frac{1}{\mathrm{i}k_m} \hat{u}_0 A_T + \hat{u}_2 A + \text{c.c.}, \qquad \text{(B 21)}$$

where $\hat{u}_2$ must be computed from (B 18) once U_1 is prescribed. Since this function is arbitrary up to the conditions in (B 7) and (B 8), $\hat{u}_2$ contains information on how U_1 is fixed. In other words, this part of the solution for u_2 will contribute to a term in the amplitude equation containing a free parameter. For this reason, we need not specify the form of $\hat{u}_2$ explicitly. This is also true of some of the terms that appear at higher order.

B.3. *Order* ϵ^2

$$yu_{2x} + v_2 + \frac{1}{F_0^2} h_{2x} = -u_{1T} - U_2 u_{0x} - U_2' v_0 - U_1 u_{1x} - U_1' v_1 + \frac{f_1}{F_0^4} h_{1x} - \frac{f_1^2}{F_0^6} h_{0x} - u_0 u_{0x} - v_0 u_{0y}, \qquad \text{(B 22)}$$

$$yv_{2x} + \frac{1}{F_0^2} h_{2y} = -v_{1T} - U_2 v_{0x} - U_1 v_{1x} + \frac{f_1}{F_0^4} h_{1y} - \frac{f_1^2}{F_0^6} h_{0y} - u_0 v_{0x} - v_0 v_{0y} \qquad \text{(B 23)}$$

and

$$yh_{2x} + u_{2x} + v_{2y} = -h_{1T} - U_2 h_{0x} - U_1 h_{1x} - (h_0 u_0)_x - (h_0 v_0)_y. \qquad \text{(B 24)}$$

In this order the nonlinear terms appear. These are problematic because, through resonance, they force other modes in the system. But, provided the harmonic, $\exp(2\mathrm{i}k_m x)$, is non-resonant, that part of the solution for u_2 is bounded (the bothersome nonlinear couplings lie at higher order in the expansion). However, a solvability condition must be enforced on the terms proportional to $\exp(\mathrm{i}k_m x)$ in (B 22)–(B 24); these terms are denoted by the superscript (1).

In order to apply solvability, first write an equation for u_2: (B 22)–(B 24) lead to the potential vorticity equation

$$-y(u_{2y}^{(1)} - v_{2x}^{(1)} - h_2^{(1)} - U_2' h_0 - U_1' h_1)_x \equiv y q_{2x}^{(1)} = U_2'' v_0 + U_1'' v_1 + (\partial_T + U_1 \partial_x) q_1, \qquad \text{(B 25)}$$

https://doi.org/10.1017/S0022112099004279 Published online by Cambridge University Press

or

$$q_2^{(1)} = \frac{1}{y}U_2''\psi_0 + \frac{1}{y}U_1''\psi_1 + \frac{1}{\mathrm{i}k_m y}(\partial_T + U_1\partial_x)q_1. \tag{B 26}$$

It is in this equation that critical-level problems appear. The right-hand side is singular as $y \to 0$, signifying $q_2^{(1)}$ diverges. On continuing,

$$\begin{aligned}\mathscr{L}u_2^{(1)} = &-[q_2^{(1)} + U_2'h_0 + U_1'h_1]_y - k_m^2 f_1 y^2 u_1 + 2\mathrm{i}k_m F_0^2 y(\partial_T + \mathrm{i}k_m U_1)u_1 - k_m^2 F_0^2 y U_1'\psi_1 \\ &+F_0^2(\partial_T + \mathrm{i}k_m U_1)^2 u_0 + \mathrm{i}k_m F_0^2 U_1'(\partial_T + \mathrm{i}k_m U_1)\psi_0 + 2k_m^2 F_0^2 y U_2 u_0 - k_m^2 F_0^2 y U_2'\psi_0.\end{aligned} \tag{B 27}$$

This equation is now multiplied by $\hat{u}_0$ and integrated over y. As in the expansion of Appendix A, however, a little care is needed because $u_2^{(1)}$ contains a jump across the critical layer. The operation leads to

$$[u_2^{(1)}(x, 0^+, T) - u_2^{(1)}(x, 0^-, T)]u_0'(0) = 2F_0^2\hat{u}_0(1)^2 A_{TT} + \mathrm{i}\Omega A_T + \Gamma A, \tag{B 28}$$

where Ω and Γ are integrals involving the solutions $\hat{u}_0$, $\hat{u}_1$ and the modifications to the profile, U_1 and U_2. Those functions are essentially arbitrary and so there is no need to give precise definitions here.

B.4. *Inner solution and matching*

The inner layer is resolved as before; pose $y = \epsilon Y$ as an inner coordinate and follow a different expansion. To the first few orders, h and v are independent of Y, and the leading-order part of u is a linear function of Y. These solutions are consistent with the inner limits of the outer solution, and matching is established straightforwardly.

The important equations arise at order ϵ and combine into the potential vorticity equation:

$$q_{IT} + Y q_{Ix} + V_0 q_{IY} - \nu q_{IYY} = U_{10}''' V_0 Y + U_{20}'' V_0, \tag{B 29}$$

where $V_0 = V_0(X, T)$ is the leading-order term of v.

For large Y, (B 29) implies the balance $q_{Ix} \sim U_{10}''' V_0$. This 'constant' is again subtracted from the critical-layer potential vorticity to obtain the part which is localized to this inner region: $q_{Ix} = \zeta_x + V_0 U_{10}'''$. With this definition, the critical-layer equation becomes

$$\zeta_T + Y\zeta_x + \Psi_x\zeta_Y - \nu\zeta_{YY} = -U_{10}'''\Psi_T + U_{20}''\Psi_x, \tag{B 30}$$

where $\Psi_x = V_0$.

Finally, the solutions for u must be matched. The procedure is similar to that described in Appendix A (and again the expansion should strictly include $\epsilon\log\epsilon$ terms), though here the expansion is carried to higher order. The results indicate that

$$u_2(x, 0^+, T) - u_2(x, 0^-, T) = -\int_{-\infty}^{\infty}\zeta(x, Y, T)\mathrm{d}Y. \tag{B 31}$$

Also, matching of v implies that $\Psi = A(T)\hat{\psi}_0(0)\mathrm{e}^{\mathrm{i}k_m x} + \text{c.c.}$ If one now selects $2F_0^2\hat{u}_0(1)^2 = 1$, rescales ζ by $-\hat{u}_0'(0)$, and defines $\kappa = -\hat{u}_0'(0)U_{10}'''$ and $\gamma = \hat{u}_0'(0)U_{20}''$, then one recovers the amplitude equations in (6.1)–(6.3). The only other point that is worth noting is that if $U(y)$ is anti-symmetrical (as in the examples of the main text), then $\Omega = \gamma = 0$.

https://doi.org/10.1017/S0022112099004279 Published online by Cambridge University Press

REFERENCES

Balmforth, N. J. 1998 Stability of vorticity defects in viscous shear. *J. Fluid Mech.* **357**, 199–224.

Balmforth, N. J. & Young, W. R. 1997 Longwave instability in shear flows. *Phys. Rev. Lett.* **79**, 4155–4159.

Blumen, W. 1970 Shear layer instability of an inviscid compressible fluid. *J. Fluid Mech.* **40**, 769–781.

Blumen, W., Drazin, P. G. & Billings, D. F. 1975 Shear layer instability of an inviscid compressible fluid. Part 2. *J. Fluid Mech.* **71**, 305–316.

Broadbent, E. G. & Moore, D. W. 1979 Acoustic destabilization of vortices. *Phil. Trans. R. Soc. Lond.* **290** A 353–371.

Case, K. M. 1960 Stability of inviscid plane Couette flow. *Phys. Fluids* **3**, 143–148.

del Castillo-Negrete, D. 1998 Nonlinear evolution of perturbations in marginally stable plasmas. *Phys. Lett.* A **241**, 99–104.

Cash, J. R. & Singhal, A. 1982 High order method for the numerical solution of two-point boundary value problems. *BIT* **22**, 184–188.

Churilov, S. M. 1989 The nonlinear stabilization of a zonal shear flow instability. *Geophys. Astrophys. Fluid Dyn.* **46**, 159–175.

Churilov, S. M. & Shukhman, I. G. 1987 The nonlinear development of disturbances in a zonal shear flow. *Geophys. Astrophys. Fluid Dyn.* **38**, 145–175.

Coullet, P. & Spiegel, E. A. 1983 Amplitude equations for systems with competing instabilities. *SIAM J. Appl. Maths* **43**, 776.

Crawford, J. D. & Hislop, P. D. 1989 Application of the method of spectral deformation to the Vlasov-Poisson system. *Ann. Phys.* **189**, 265–317.

Drury, L. O'C. 1985 Acoustic amplification in discs and tori. *Mon. Not. R. Astron Soc.* **217**, 821–829.

Farrell, B. F. 1982 The initial growth of disturbances in a baroclinic flow. *J. Atmos. Sci.* **39**, 1663–1686.

Fjørtoft, R. 1950 Application of integral theorems in deriving criteria of stability of laminar flow and for the baroclinic circular vortex. *Geofys. Publ.* **17**, 1–52.

Ford, R. 1994 The instability of an axisymmetric vortex with monotonic potential vorticity in rotating shallow water. *J. Fluid Mech.* **280**, 303–334.

Glatzel, W. 1985 Sonic instabilities in supersonic shear flows. *Mon. Not. R. Astron. Soc.* **231** 795–821.

Glatzel, W. 1989 The linear stability of viscous compressible plane Couette flow. *J. Fluid Mech.* **202**, 515–541.

Goldstein, M. E. & Hultgren, L. S. 1988 Nonlinear spatial evolution of an externally excited instability wave in a free shear layer. *J. Fluid Mech.* **197**, 295–330.

Goldstein, M. F. & Leib, S. J. 1988 Nonlinear roll-up of externally excited free shear layers. *J. Fluid Mech.* **191**, 481–515.

Griffiths, R. W., Killworth, P. D. & Stern, M. E. 1982 A geostrophic instability of ocean currents. *J. Fluid Mech.* **117**, 343–377.

Guckenheimer, J. & Holmes, P. 1983 *Nonlinear Oscillations, Dynamical Systems, and Bifurcations of Vector Fields*. Springer.

Hayashi, Y.-Y. & Young, W. R. 1987 Stable and unstable shear modes of rotating parallel flows in shallow water. *J. Fluid Mech.* **184**, 477–504.

Knessl, C. & Keller, J. B. 1992 Stability of rotating shear flows in shallow water. *J. Fluid Mech.* **244**, 605–614.

Kubokawa, A. 1985 Instability of a geostrophic front and its energetics. *Geophys. Astrophys. Fluid Dyn.* **33**, 223–257.

Lin, C. C. 1945 On the stability of two-dimensional parallel flows. *Q. Appl. Maths* **3,** 117–142, 218–234, 277–301.

Narayan, R., Goldreich, P. & Goodman, J. 1987 Physics of modes in a differentially rotting system – analysis of the shearing sheet. *Mon. Not. R. Astron. Soc.* **228**, 1–41.

Papaloizou, J. C. B. & Pringle, J. E. 1987 The dynamical stability of differentially rotating discs-III. *Mon. Not. R. Astron. Soc.* **225**, 267–283.

Perkins, J. & Renardy, M. 1997 Stability of equatorial currents with nonzero potential vorticity. *Geophys. Astrophys. Fluid Dyn.* **85**, 31–64.

https://doi.org/10.1017/S0022112099004279 Published online by Cambridge University Press

Rayleigh, Lord 1880 On the stability, or instability, of certain fluid motions. *Proc. Lond. Math. Soc.* **9**, 57–70.

Ripa, P. 1983 General stability conditions for zonal flows in a one-layer model on the β-plane or the sphere. *J. Fluid Mech.* **126**, 463–489.

Satomura, T. 1981 An investigation of shear instability in a shallow water. *J. Met. Soc. Japan* **59**, 148–167.

Shukhman, I. G. 1991 Nonlinear evolution of spiral density waves generated by the instability of the shear layer in a rotating compressible fluid. *J. Fluid Mech.* **233**, 587–612.

Stewartson, K. 1978 The evolution of the critical layer of a Rossby wave. *Geophys. Astrophys. Fluid Dyn.* **9**, 185–200.

Stewartson, K. 1981 Marginally stable inviscid flows with critical layers. *IMA J. Appl. Maths* **27**, 133–175.

Takehiro, S.-I. & Hayashi, Y. Y. 1992 Over-reflection and shear instability in a shallow-water model. *J. Fluid Mech.* **236**, 259–279.

Warn T. & Warn, H. 1978 The evolution of a nonlinear critical level. *Stud. Appl. Maths* **59**, 37–71.

Williams, J. S. 1992 Nonlinear problems in vortex sound. PhD Thesis, University of Leeds.

https://doi.org/10.1017/S0022112099004279 Published online by Cambridge University Press